Russian Chemical Reviews **74** (4) 317 – 337 (2005) © 2005 Russian Academy of Sciences and Turpion Ltd

DOI 10.1070/RC2005v074n04ABEH000892

The use of selective methods of heteronuclear NMR spectroscopy in studies of multicomponent systems †

Yu E Chernysh, V A Volynkin, V T Panyushkin, V I Kondakov, M S Korobov, G S Borodkin

Contents

I.	Introduction	317
II.	Selective pulses	318
III.	Pulsed magnetic field gradients	318
IV.	Selective methods with inverse detection	319
V.	Measurements of self-diffusion coefficients	326
VI.	Observation of 'underwater' signals. RECUR NMR technique	328
VII.	Homonuclear selective methods	329
VIII.	Heteronuclear experiments	332
IX.	Two-dimensional correlation experiments based on heteronuclear *J*-cross-polarisation	334
X.	Combined use of selective and non-selective excitation in NMR experiments	334

Abstract. Some important aspects of the use of selective methods in NMR spectroscopy for interpreting the spectra of complex multicomponent systems, measuring the spin – spin coupling constants and determining the structure of compounds are discussed. Procedures for recording selective spectra and the application of selective radiofrequency pulses together with magnetic field gradient pulses are described. Practical methods for suppression of water signals in the study of biological samples are considered. The bibliography includes 198 references.

I. Introduction

NMR spectroscopy belongs to the most efficient methods of investigation of the liquid, solid and liquid-crystalline states of matter.[1] Correctly interpreted NMR spectra give a clear picture of the molecular conformations, internuclear and intermolecular distances, angles and bond properties and information on the molecular dynamics. Usually, the most significant information is extracted from three main parameters of an NMR spectrum, namely, the chemical shift, spin – spin coupling constant and nuclear spin relaxation rate.[2–6] However, these parameters cannot always be measured immediately from the spectrum. This is due to low sensitivity of NMR spectroscopy owing to very small transition energy differences ($\sim 10^{-6}$ eV) between nuclear energy levels and to the low natural abundance and gyromagnetic ratios of many nuclei. Often, these factors act in line with one another.

Yu E Chernysh, M S Korobov, G S Borodkin Institute of Physical and Organic Chemistry of the Rostov State University, prosp. Stachki 194/2, 344090 Rostov-on-Don, Russian Federation. Fax (7-8632) 43 46 67, tel. (7-8632) 43 38 94, e-mail: nmr@ipoc.rsu.ru
V A Volynkin, V T Panyushkin Kuban State University, Stavropolskaya ul. 149, 350040 Krasnodar, Russian Federation. Fax (7-8612) 69 95 70, tel. (7-8612) 69 95 74, e-mail: vva@chem.kubsu.ru (V A Volynkin), Panyushkin@chem.kubsu.ru (V T Panyushkin)
V I Kondakov Grodno State Agrarian University, ul. Tereshkovoi 28, 230008 Grodno, Belarus. Fax (37-5152) 77 01 68, tel. (37-5152) 72 00 24, e-mail: Vlad.Kondakov@mail.ru

Received 19 August 2004
Uspekhi Khimii **74** (4) 344 – 368 (2005); translated by A M Raevskiy

Yet another problem consists of the overlap of resonance signals, which is particularly typical of the spectra of large molecules and complex systems. As an example, let us compare resonances of two widely used nuclei, ^{1}H and ^{13}C. ^{1}H NMR spectroscopy is characterised by higher sensitivity due to both high natural abundance of the ^{1}H isotope (99.98%) and high gyromagnetic ratio [26.75 rad (s T)$^{-1}$]. However, the width of the ^{1}H NMR spectrum is about 20 ppm while signals of most organic compounds are observed in an interval of around 8 ppm. ^{13}C resonances are observed in a much wider region of chemical shifts (200 ppm), signals being relatively well-resolved. However, the natural abundance of this isotope is low (1.1% of the total content of carbon isotopes) and its gyromagnetic ratio is low (0.25 of the gyromagnetic ratio of the ^{1}H isotope). Therefore, ^{13}C NMR spectroscopy is less sensitive. Using higher magnetic fields allows the sensitivity and resolution to be enhanced. However, ^{1}H NMR spectra of complex samples (*e.g.*, biological liquids and tissue extracts) remain overcrowded even at a frequency of 800 MHz,[7] such ultrahigh-field systems being too expensive. An alternative approach to enhancement of the sensitivity and spectral resolution is based on design of new pulse sequences for selective detection of particular signals.

At present, NMR methodology concerns not only the known and continuously revisable two-dimensional (2D) and three-dimensional (3D) pulse methods but also two more avenues. One of them is associated with the use of selective radiofrequency (RF) pulses[8–10] while the other employs pulsed magnetic field gradients (PFG), which improve the spectra by selecting appropriate coherent superpositions of different states of the nuclear spin system (from this point on, coherences).[11–13] Both methods, their advantages and drawbacks have been well documented.[8–13] Often, methods based on the use of selective RF pulses only are complicated by artifacts arising from long pulse durations. To suppress unwanted responses, phase cycling is needed. Experiments with selective pulses require a skilled operator; interpretation of the resulting spectrum is often unobvious and therefore the corresponding techniques are of limited use. In the case of PFG, no phase cycling is needed and the duration of experiments is

† Dedicated to Academician Vladimir Minkin on the occasion of his 70th birthday.

shortened by a factor of nearly five. The most promising approaches combine both these methods.[14, 15]

Combining selective RF pulses and pulsed field gradients began only recently but this gave good results.

II. Selective pulses

The function of selective pulses[8–10] is to excite or invert certain resonances, either singlets or multiplets (sometimes, these can be subspectra within the same spectrum or single lines within a multiplet). The structure of organic compounds is determined using selective pulses, which allow the dimension of the problem to be reduced from 3D to 2D or from 2D to 1D in one experiment and necessary information to be obtained during a shorter time period with a rather high resolution.

Three general problems arise when using selective pulses. The first problem is associated with a rather long duration of such pulses, which is three orders of magnitude longer than the duration of non-selective 'hard' pulses. The selectivity obtained nearly equals the inverse pulse duration. For instance, excitation of a multiplet of spectral width 50 Hz requires a selective pulse of about $\sim$20 ms long to be applied. Eagerness for selectivity enhancement can lead to considerable relaxation loss within the pulse sequence.

The second problem concerns the shape of the selective pulse profile. An 'ideal pulse' must have a rectangular envelope uniformly filled with the carrier radiofrequency. In the framework of the consecutive response theory the excitation profile can be calculated using the direct Fourier transform of the pulse shape from the frequency domain to the time domain and *vice versa*. However, the consecutive response theory is valid only for very weak excitation; therefore, the shape design of new selective pulses, which is usually performed using iterative methods, must involve an experimental stage. The most widely used shaped pulses are shown in Fig. 1. Application of a rectangular, Gaussian and sinc-type pulse creates a sinc-type, Gaussian and rectangular excitation profile, respectively.

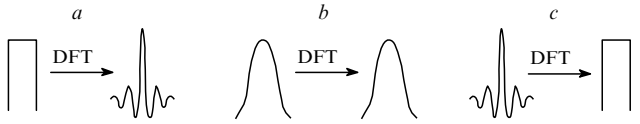


Figure 1. RF pulse shapes and corresponding excitation profiles.
Pulse: rectangular (*a*), Gaussian (*b*) and sinc (*c*); DFT stands for direct Fourier transform.

The third problem is concerned with the phase change of the selective pulse. Unfortunately, the excitation phase varies within the chosen width of a selective pulse. Therefore, excitation of a multiplet by a selective pulse can lead to a complex spectral pattern, because first-order phase correction is impossible. Pulse sequence designers mostly aim their efforts at generating short selective pulses with a constant phase and a smooth envelope within the semicircle. However, this problem has no exact solution and therefore it is necessary to find approximate solutions.

In principle, it is possible to determine the excitation profile and the phase change of the pulses employed. This requires a successive variation of the repetition frequency of a selective pulse in the frequency region of interest; however, the procedure is very time-consuming. Hwang and Shaka[16] reported an experiment with pulsed magnetic field gradients employed to 'visualise' the shape of a selective excitation pulse (Fig. 2). The pulse sequence used is inappropriate for solving structural chemical tasks; however, it exhibits many features of widely used pulse sequences. Experiments were carried out with the spin echo gradient sequence. When the selective pulse is on, a magnetic field gradient is applied to reproduce the image of the frequency distribution,

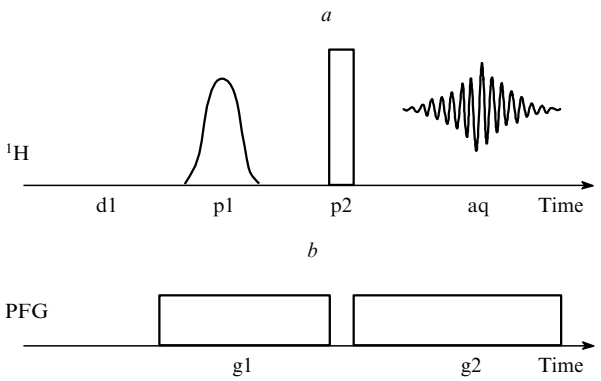


Figure 2. The RF pulse sequence (*a*) and PFG sequence (*b*) used for determination of the excitation profiles of 90° pulses.
d1 is the relaxation delay, p1 is the selective 90° pulse, p2 is the 180° pulse, g1 and g2 are the rectangular pulse gradients and aq is the acquisition time.

which is read out during the data acquisition time, *i.e.*, during the last time interval.

The phases of the 90° Gaussian and sinc pulses change their signs, whereas the semi-Gaussian pulse has good phase characteristics and a good excitation profile for the *x*-magnetisation only. BURP[15] (Band-selective Uniform Response Pure-phase Pulses) type pulses are characterised by a very good phase mode. These 'soft' pulses are designed for refocussing the magnetisation trajectory in such a way that the natural divergence between the fast and slow components of the magnetisation vector is corrected. These pulses transfer the magnetisation to the $+y$ axis in the whole range of resonance offsets, *i.e.*, shifts of the resonances from zero.

A 180° Gaussian pulse provides a good selectivity and phase mode due to the action of a REBURP (Refocused Band-selective Uniform Response Pure-phase) composite pulse. It should be noted that old spectrometers having no envelope shape storage modules can operate with modern pulses that can be programmed using the DANTE (Delays Alternating with Nutation for Tailored Excitation) sequence.[17, 18]

Prior to using selective pulses, the operator has to calibrate the excitation profiles. A detailed description of calibration procedures was reported by Braun *et al.*[19] The procedures are much like those used in the calibration of 'hard' pulses. The main difference is that determination of the duration of the 180° pulse only requires damping of the RF power. One should keep in mind that damping 'operates' in the logarithmic scale. Therefore, experiments with old instruments, which have no software for matching the initial phases of pulses within the same pulse sequence, require a check of either the phase of the selective 90° RF pulse or, at least, the phase of the 90° pulses with the phases of 'hard' 90° pulses at the same power. If both pulses are applied within the same pulse sequence, the difference in the corresponding phase programme must be set every time.

III. Pulsed magnetic field gradients ‡

Selection of coherences using pulsed magnetic field gradients has been studied in detail.[11–13] The field gradient applied along the *z* axis causes a *z*-dependence of the resonance frequencies and thus the phase dependence of the magnetisation (Fig. 3). If the gradient

‡ The abbreviations of the NMR techniques employing pulsed magnetic field gradients are as follows: GRASP (Gradient Accelerated Spectroscopy) and ge (gradient enhanced). It is more appropriate to use the gs (gradient selection) abbreviation, which has been commonly accepted. Actually, the magnetic field gradients 'select' desired and 'ignore' undesired coherences; therefore, this term seems to be the best to reflect the essence of all the known gradient experiments.

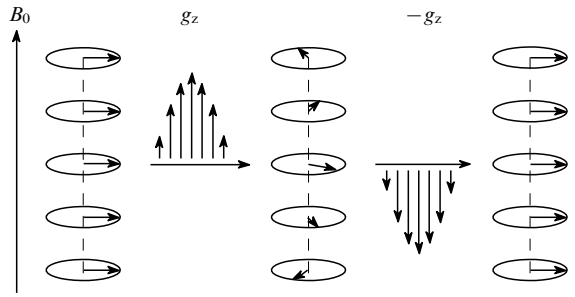


Figure 3. The action of pulsed magnetic field gradient.
Application of the gradient g_z causes dephasing, which is rephased by applying the gradient $-g_z$.

pulse has a limited intensity and duration, switching it off will be followed by precession of identical spins at their initial frequencies with the gradient-set phases. A signal detected at this stage will at best have the shape of a broadened absorption signal. Applying the second field gradient pulse of the opposite sign will result in a conventional NMR spectrum. Therefore, dephasing caused by the first gradient can be rephased by applying the second gradient, which is identical to the first one but has the opposite sign.

Practical implementation of this principle offers great prospects. Dephasing and rephasing depend on the gyromagnetic ratio and coherence orders at the instant of application of the gradient pulse; therefore, one can readily select coherences by changing their orders between the gradients set by the RF pulses. If selective RF pulses are applied between two gradients, only the coherences created by these pulses contribute to the resulting signal.

The use of magnetic field gradient pulses can be best considered using the coherence transfer diagram, which is based on the shift operators I^+ and I^-. From the expression

$$I_x = \frac{1}{2}(I^+ + I^-) \tag{1}$$

it can be seen that the excitation by a 90° pulse can cause both a decrease and an increase in the coherence level (Fig. 4).

In performing a theoretical description it is assumed that the NMR spectrometers set the I^- level. Therefore, the RF pulses for detection using a pulse sequence must be chosen in such a way that the coherence trajectory arrives at this level. Here, the field gradient pulses must be distributed in a fashion that excludes other possible trajectories. To select the desired coherence, the following condition must be met:

$$\sum_{i=1} p_i \gamma_i g_i \geqslant 0, \tag{2}$$

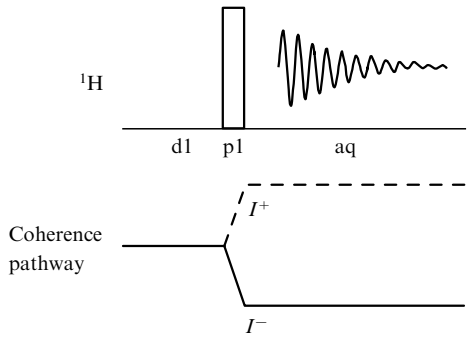


Figure 4. Coherence pathway diagram for the excitation by a single RF pulse.

where p_i is the order of the ith coherence, a γ_i is the effective gyromagnetic coefficient, which exists during the action of ith pulse gradient g_i. All gradient pulses are assumed to have the same duration and shape.

Figure 5 presents a typical result of the gradient strength measurements using the pulse sequence shown in Fig. 6. The possibility of using the field gradient pulses depends on the degree of improvement of the spectrometer hardware.

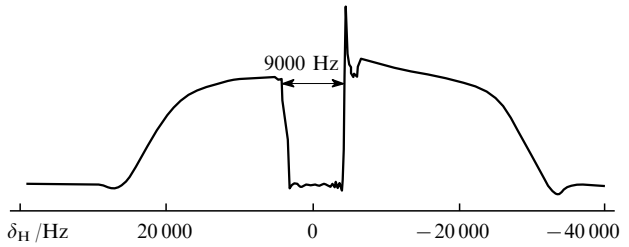


Figure 5. Results of measurements of the magnetic field gradient strength in a water sample (a Teflon disk of diameter 2 mm was placed at the centre of the sample);[18]
δ_H is the chemical shift of protons.

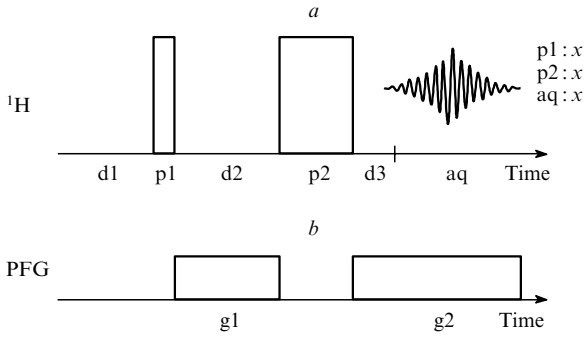


Figure 6. The RF pulse sequence (*a*) and PFG sequence (*b*) used for determination of the magnetic field gradient strength.
For notations, see Fig. 2.

IV. Selective methods with inverse detection

Usually, the function of selective methods is to determine the structure of organic compounds. Below we will consider only the $^{13}C-^1H$ groups (though other groups, *e.g.*, NH, NH_2 and NH_3 can also be considered). There are five main types of spin systems, namely, those of methyl ($^{13}CH_3$), methylene ($^{13}CH_2$) and methyne (^{13}CH) groups, quaternary ^{13}C atoms and all protons attached to ^{12}C, O, N, *etc.* rather than ^{13}C. The multiplicity of the ^{13}C resonances depends on the number of attached protons. Because of this, particular $^{13}CH_n$ groups are characterised by different precession rates of scalar coupling, possible highest orders of multiquantum coherences and corresponding angles and phases of RF pulses. These features are used in spectral editing for selective detection of ^1H and ^{13}C signals. At present, spectral editing is used in ^{13}C NMR spectroscopy as a routine technique for assignment of C, CH, CH_2 and CH_3 signals.

Pulse methods comprise the APT (Attached Proton Test),[20–23] SEMUT (Subspectral Editing Using a Multiple-Quantum Trap),[24,25] RELAY (Relayed Correlation Spectroscopy),[26,27] INEPT (Insensitive Nuclei Enhanced by Polarisation Transfer),[28,29] DEPT (Distortionless Enhancement by Polarisation Transfer)[30–32] and PENDANT (Polarisation Enhancement During Attached Nucleus Testing)[33] techniques. An important role in spectral editing is played by various J precession effects in CH_n groups. For instance, in the INEPT

experiments the signal intensities of different CH_n groups depend on time and J precession angle, which is proportional to the number, n, of attached protons. In the case of the DEPT pulse sequence spectral editing is performed using specific angles of the coherence transfer pulses that are applied on double-quantum and zero-quantum coherences containing a total of $n+1$ spins.

In these methods, the magnetisation is transferred from ^1H to ^{13}C and theoretically the sensitivity of the ^{13}C nuclei must increase by a factor of four[2] due to both pre-saturation of ^1H-coherences[21,22] and the use of different pulse sequences.[26–33] In addition, the pulse sequences creating the transfer of ^1H-polarisation are used in 2D heteronuclear correlation experiments,[34] in which the proton and carbon signals are in the F_1 and F_2 dimensions, respectively.

A large number of communications on the use of heteronuclear filtering for simplification of ^1H NMR spectra has been reported in the last decade.[35–50] One of these methods is known as inverse detection NMR spectroscopy or NMR spectroscopy with proton detection. It is characterised by high sensitivity, because of the use of ^1H nuclei with high gyromagnetic ratio for both coherence creation and detection.[4]

Heteronuclear single-quantum or multiquantum coherences are incorporated in the middle of most of the pulse sequences based on the INEPT and DEPT with inverse signal detection (inverse DEPT and inverse INEPT).[35–37]

The RELAY pulse sequence[38] uses two 90° (^1H) pulses for selective excitation of $^{13}CH_n$ group coherences.[26,27]

Using specific methods, one can easily obtain ^1H NMR subspectra of $^{13}CH_2$ (^{13}CH or $^{13}CH_3$) groups only. Obtaining the spectrum of ^{13}CH groups is a non-trivial task because the ^{13}CH and $^{13}CH_3$ spin systems have the same phases. A method for recording selective spectra of $^{13}CH_n$ groups with minimum phase and intensity distortions was proposed.[46] It is based on the principle of Quantum Filtering of Maximum Order (MAXY).[43–47] In the MAXY experiments the spin systems of $^{13}CH_n$ groups are excited to corresponding maximum possible (for a given group) order of heteronuclear multiquantum coherence (second order for ^{13}CH, third order for $^{13}CH_2$ and fourth order for $^{13}CH_3$). This provides the possibility of selective observation of signals of one, two or all three groups. Selectivity can be achieved by using both phase cycling and pulsed field gradients.

1. DEPT and INEPT experiments

The possibility of editing the spin system in the DEPT and INEPT experiments is attained by using a corresponding angle for one pulse in the DEPT sequence or the precession angle $\pi J\tau$ (J is the spin–spin coupling constant and τ is the time interval between pulses) of the heteronuclear coupling in the INEPT experiments. The pulse angles ($\psi = \beta$, DEPT) and precession angles ($\psi = \pi J\tau$, INEPT) affect the signal intensities of different $^{13}CH_n$ groups. The signal intensity depends on $\sin(\psi)$ for ^{13}CH, on $\sin(2\psi)$ for $^{13}CH_2$ and on $(3/4)(\sin3\psi + \sin\psi)$ for $^{13}CH_3$. Analogous principles are implemented in the DEPT and INEPT methods with inverse detection.

By specifying the delays and pulse angles and using the inverse-DEPT or inverse-INEPT sequences, a number of spectra are obtained. Then, by subtracting (adding) the spectra one gets the edited spectra of $^{13}CH_n$ groups; however, the signal intensities become distorted (Table 1).

In the inverse-DEPT sequence (Fig. 7), the β_y pulse is applied to heteronuclear zero-quantum and double-quantum coherences $2S_yI_x$ (^{13}CH), $4S_xI_xI_z$ ($^{13}CH_2$) and $8S_yI_xI_zI_z$ ($^{13}CH_3$) and the products of the operators, which remain the same as before application of the β_y pulse, contribute to the signals observed.

The dependences of the signal intensities of the groups mentioned above are as follows:
for ^{13}CH groups

$$2S_yI_x \xrightarrow{\beta_y} 2S_yI_x\cos\beta, \qquad (3)$$

Table 1. Combination of NMR spectra for obtaining ^1H subspectra of individual $^{13}CH_n$ groups using the inverse DEPT sequence with the pulse angles $\beta = 60°$ (I), 120° (II) and 180° (III).[35–37]

Spin system	Signal intensity (rel.u.)			Combination	Intensity ratio	Number of runs
	I	II	III			
^{13}CH	0.5	−0.5	−1.0	0.111(I) − II − −0.555 (III)	1.0	3
$^{13}CH_2$	−1.0	−1.0	2.0	I + II	2.0	2
$^{13}CH_3$	−1.875	1.875	−3.0	I + 0.5 III	3.3	2

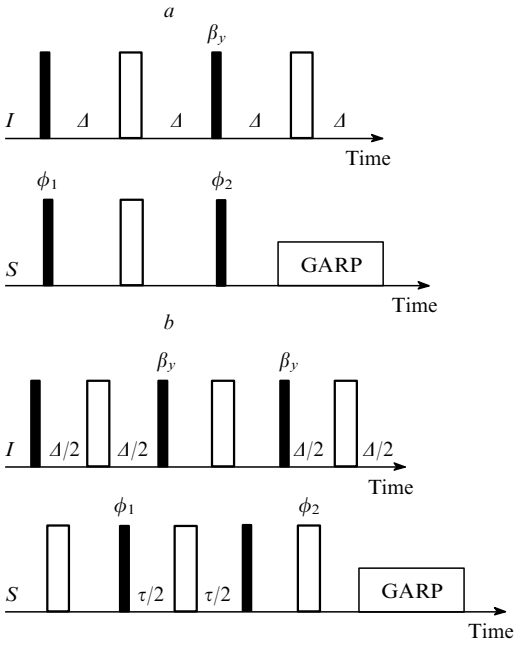


Figure 7. The inverse DEPT (*a*) and inverse INEPT (*b*) pulse sequences. I and S are the spins of a coupled system IS; Δ are the time intervals between pulses; β_y is the pulse applied along the y axis; ϕ_1 and ϕ_2 are the flip angles for the first and second pulse, respectively; GARP are the Globally-optimised, Alternating-phase Rectangular Pulses for Broadband Decoupling.
Here and in Figs 9–14, 16, 18, 20–22, 24, 26 and 27 the filled and open rectangles denote the 90° and 180° pulses, respectively.

for $^{13}CH_2$ groups

$$4S_xI_xI_z \xrightarrow{\beta_y} 4S_xI_xI_z\cos2\beta,$$

and for $^{13}CH_3$ groups

$$-8S_yI_xI_zI_z \xrightarrow{\beta_y} -2S_yI_xI_zI_z(3\cos3\beta + \cos\beta).$$

When using the inverse-INEPT sequence and the spin–spin interaction Hamiltonian in the form $\pi J_{IS}\tau(2S_yI_z)$ (J_{IS} is the spin–spin coupling constant between nuclei with the spins I and S), intensity modulation occurs during the interval τ in the middle of the pulse sequence. The expressions for the signals observed before and after the evolution of the system caused by the spin–spin interaction have the form:
for ^{13}CH

$$2S_yI_x \xrightarrow{\pi J\tau(2S_yI_z)} 2S_yI_z\cos\psi, \qquad (4)$$

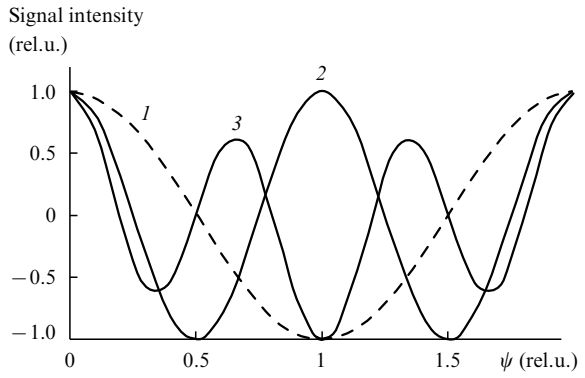


Figure 8. ^{13}CH (*1*), $^{13}CH_2$ (*2*) and $^{13}CH_3$ (*3*) signal intensities plotted *vs.* pulse angle β (inverse DEPT) (*1*), evolution time τ (inverse INEPT) (*2*) and pulse phase ϕ_2 (MAXY) (*3*).

for $^{13}CH_2$

$$2\,S_yI_z \xrightarrow{\pi J\tau(2\,S_yI_z)} 2\,S_yI_z\cos2\psi,$$

and for $^{13}CH_3$

$$2\,S_yI_x \xrightarrow{\pi J\tau(2\,S_yI_z)} 2\,S_yI_z\frac{1}{4}(\cos3\psi+\cos\psi).$$

Figure 8 presents the signal intensities of different spin systems plotted *vs.* the relative pulse angle ($\psi = \beta$, inverse-DEPT), evolution time ($\psi = \tau$, inverse-INEPT) and pulse phase ($\psi = \phi_2$, MAXY). Signals of the ^{13}CH, $^{13}CH_2$ and $^{13}CH_3$ groups can be separated using the 60°, 120° and 180° pulses, respectively (inverse-DEPT), or the evolution times equal to $1/3J$, $2/3J$ and $1/J$, respectively (inverse-INEPT).

2. Selective experiments based on the MAXY sequence

The MAXY sequence (Fig. 9 *a*) includes excitation of the spin ($^{13}CH_n$) systems to the maximum possible quantum order using the following pulse scheme: $90^\circ_x(I)-\Delta-90^\circ_x(S)180^\circ_x(I)-\Delta-90^\circ_x(I)$ (where $\Delta = 1/2J$).[46,47]

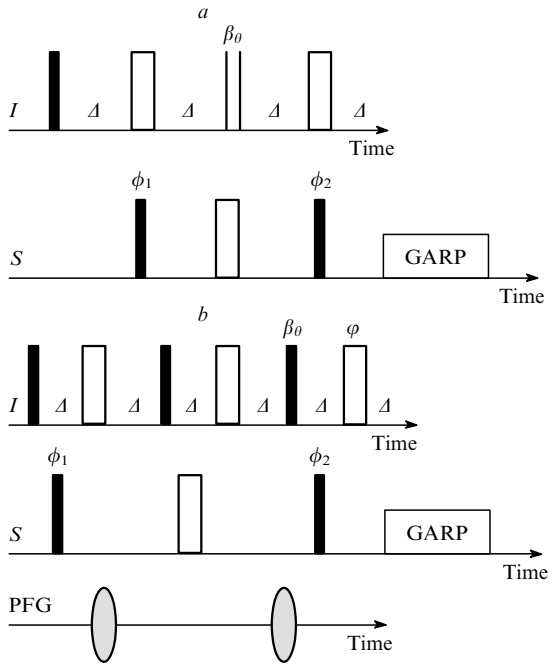


Figure 9. MAXY pulse sequence without (*a*) and with PFG (*b*).

Since the maximum possible quantum level of each different spin system is different, it is possible to convert all transitions, or any transition, to observable ^1H single-quantum coherence. Spectral editing can be achieved by using multiple-quantum proton read pulses with different phases (θ) as in, *e.g.*, the RELAY sequence[26,27] or different flip angles (β) as in the DEPT sequence.[30,31] But it is also possible to use simply *pm x*- or $\pm y$-phases (*i.e.*, phases associated with the positive or negative direction of the pulses along the coordinate axes) because this provides the highest signal intensity.

a. Spectral selection using phase cycling

When using a sequence of $90^\circ_\theta(I)-\Delta-90^\circ_{\phi_2}(S)180^\circ_\varphi(I)-\Delta$ ($\varphi = \theta/2$) all multiple-quantum coherences can be converted to observable magnetisation:[47]

for ^{13}CH

$$+2\,I_xS_y \xrightarrow{90^\circ_\theta-\Delta-180^\circ_\phi(I)90^\circ_{\phi_2}(S)-\Delta} I_y\cos\theta, \qquad (5)$$

for $^{13}CH_2$

$$+2\,I_xI_yS_x \xrightarrow{90^\circ_\theta-\Delta-180^\circ_\phi(I)90^\circ_{\phi_2}(S)-\Delta} I_y\cos2\theta,$$

and for $^{13}CH_3$

$$-8\,I_xI_yI_yS_y \xrightarrow{90^\circ_\theta-\Delta-180^\circ_\phi(I)90^\circ_{\phi_2}(S)-\Delta} (1/4)\,I_y(3\cos3\theta+\cos\theta).$$

The pulse $90^\circ(I_\theta)$ converts part of the magnetisation to zero-quantum and double-quantum coherences with intensities proportional to $\cos n\theta$. The expression for a $^{13}CH_3$ group contains two terms proportional to $\cos3\theta$ and $\cos\theta$ with intensity ratios of 3 : 1, respectively, and which correspond to the ^1H triple-quantum coherence of $8\,I_xI_yI_y$. The desired resonances can be selected by phase cycling the $90^\circ(\theta)$ pulse with $\theta = 180^\circ/n$, where n is the number of attached protons. An advantage in this procedure is that resonances of protons not bound to ^{13}C can be better suppressed by further cycling of the receiver phase. The phase cycling programmes for selection of $^{13}CH_2$ and $^{13}CH_3$ resonances *via* ^1H double-quantum and triple-quantum coherences are listed in Table 2.

Table 2. Phase cycling programmes for selective observation of $^{13}CH_2$ and $^{13}CH_3$ resonances with the MAXY sequence.

Phase	For $^{13}CH_2$	Phase	For $^{13}CH_3$
ϕ_1	0°, 180°	ϕ_1	0°, 180°
ϕ_2	0°, 0°, 180°, 180°	ϕ_2	0°, 0°, 180°, 180°
θ	$(0^\circ)_4$, $(90^\circ)_4$, $(180^\circ)_4$, $(270^\circ)_4$	θ	$(0^\circ)_4$, $(60^\circ)_4$, $(120^\circ)_4$, $(180^\circ)_4$, $(240^\circ)_4$, $(300^\circ)_4$
ϕ	$(0^\circ)_4$, $(45^\circ)_4$, $(90^\circ)_4$, $(135^\circ)_4$	ϕ	$(0^\circ)_4$, $(30^\circ)_4$, $(60^\circ)_4$, $(90^\circ)_4$, $(120^\circ)_4$, $(150^\circ)_4$
ϕ_n	0°, 180°, 180°, 0°, 180°, 0°, 0°, 180°	ϕ_r	0°, 180°, 180°, 0°,180°, 0°, 0°, 180°

Note. The subscripts denote the numbers of cycles.

It is interesting that mathematical expressions for the observable signals for the inverse-DEPT, inverse-INEPT and MAXY sequences have the same form [see Eqns (4) and Fig. 8].

It is possible to obtain subspectra of the CH_3 and CH_2 groups by choosing appropriate ϕ values (see Table 2). This can be done by phase cycling in the MAXY experiments because the variable is the read pulse phase (θ). When using inverse-DEPT and inverse-INEPT methods, the variables are the pulse flip angles and times, respectively, and the task becomes much more complicated.

Table 3. Combination of NMR spectra for obtaining ^{1}H subspectra of individual $^{13}CH_n$ groups using the MAXY sequence with the pulse angles $\beta = 0^\circ$ (I), 90° (II), 270° (III).[43–47]

Spin system	Signal intensity (rel. u.)					Combination of spectra	Intensity ratio	Number of runs
	I	II	III	II + III	II − III			
^{13}CH	1	1	1	1	0	I	1.0	1
$^{13}CH_2$	0	2	−2	0	2	II − III	2.0	1
$^{13}CH_3$	0	3	3	3	0	II + III − I	3.0	2

b. Spectral selection using a $\beta_x(I)$ pulse

If a $\beta(I)$ pulse is applied along the x axis, it will convert part of the magnetisation heteronuclear zero-quantum and double-quantum coherence, which is then transferred to I-spin single-quantum coherence by the pulse following a delay Δ. The data acquisition starts after a delay of Δ and results in in-phase (correct) absorption lineshapes for all spins with the intensities proportional to $\sin\beta$ (for $^{13}CH_2$) or $\sin^2\beta$ (for $^{13}CH_3$); the exception is the ^{13}CH group, which is not affected by the $\beta_x(I)$ pulse:

for ^{13}CH

$$+2I_xS_y \xrightarrow{\beta_x(I)} +2I_xS_y \xrightarrow{\Delta - 180^\circ_x(I)90^\circ_x(S) - \Delta} +I_y, \qquad (6)$$

for $^{13}CH_2$

$$+4I_xI_yS_x \xrightarrow{\beta_x(I)} +4I_xI_zS_z\sin\beta \xrightarrow{\Delta - 180^\circ_x(I)90^\circ_x(S) - \Delta} +I_y\sin\beta,$$

for $^{13}CH_3$

$$-8I_xI_yI_yS_y \xrightarrow{\beta_x(I)} -8I_xI_zI_zS_y\sin^2\beta \xrightarrow{\Delta - 180^\circ_x(I)90^\circ_x(S) - \Delta} +I_y\sin^2\beta.$$

When studying the dependence of the signal intensities on the pulse flip angle (β_x), the flip angles of 0°, 180°, 90° and 270° are particularly interesting because at these angles the intensities reach extrema, which can be used for spectral editing. If a 0° or 180° ^{1}H read pulse is used, only ^{13}CH resonances can be observed. The efficiency of suppression of $^{13}CH_2$ and $^{13}CH_3$ signals is very high, because these groups are in the multiple-quantum coherence states and all protons not bound to ^{13}C will have only longitudinal magnetisation.

A 90° or 270° ^{1}H read pulse will convert the coherence of $^{13}CH_2$ and $^{13}CH_3$ groups to heteronuclear zero-quantum and double-quantum coherences and thus make it possible to get the true intensity (for $\beta = 90^\circ$, all signals in the spectrum are positive, whereas for $\beta = 270^\circ$, only $^{13}CH_2$ signals are negative). This provides a way to edit the spectra by phase cycling, because the 90° and 270° flip angles are equivalent to a 90° pulse with phases of x and $-x$ directions. As a result, if the receiver phase is shifted (subtraction of spectra), one gets the subspectrum of $^{13}CH_2$ groups only; otherwise if the receiver phase is fixed (addition of spectra), the subspectrum of ^{13}CH and $^{13}CH_3$ groups together is observed.

c. Spectral selection using a $\beta_y(I)$ pulse

Yet another method of obtaining the ^{13}CH and $^{13}CH_2$ subspectra involves the use of a $\beta(I)$ read pulse applied only along the y axis. The effect of such a pulse is shown in Eqns (7):

for ^{13}CH

$$+2I_xS_y \xrightarrow{\beta_y(I)} +2I_xS_y \xrightarrow{\Delta - 180^\circ_x(I)90^\circ_x(S) - \Delta} +I_y\cos\beta, \qquad (7)$$

for $^{13}CH_2$

$$+4I_xI_yS_x \xrightarrow{\beta_y(I)} +4I_xI_zS_z\sin\beta \xrightarrow{\Delta - 180^\circ_x(I)90^\circ_x(S) - \Delta} +I_x\sin\beta,$$

for $^{13}CH_3$

$$-8I_xI_yI_yS_y \xrightarrow{\beta_y(I)} -8I_yI_yI_zS_y\sin\beta \xrightarrow{\Delta - 180^\circ_x(I)90^\circ_x(S) - \Delta} \longrightarrow +8I_yI_yI_zS_y\sin\beta.$$

Note that the coherence of $^{13}CH_3$ groups cannot be converted to observable magnetisation by a read pulse applied along the y axis.

The intensities of ^{13}CH and $^{13}CH_2$ group resonances vary in proportion to $\cos\beta$ and $\sin\beta$, respectively. Therefore, a 90° pulse along the y axis allows the subspectrum of the $^{13}CH_2$ group to be selected. The editing scheme for MAXY ^{1}H NMR spectra using spectrum addition or subtraction with β pulses is given in Table 3.

d. The use of pulsed magnetic field gradients

An advantage of the MAXY method over the inverse-DEPT and inverse-INEPT techniques is that selective detection of resonance signals can be achieved using pulsed magnetic field gradients.[46–50] This was shown to provide enhanced performance in many pulse sequences. In the MAXY experiments, the spin systems $^{13}CH_n$ are excited to their highest possible quantum levels. In this case it is possible to observe subspectra of individual $^{13}CH_n$ groups using PFG because the phase of the multiple-quantum coherence is proportional to the quantum order of the coherence. The quantum orders of all $^{13}CH_n$ systems are the same in both the inverse-DEPT and inverse-INEPT experiments; therefore, pulsed magnetic field gradients cannot be used for selective detection. The PFG-MAXY pulse sequence is shown in Fig. 9 *b*. Here, two pulses are used, with the first one applied during the first Δ delay period and the second one applied immediately after the last $90^\circ(S)$ transfer pulse, the field gradients having the values of g_1 and g_2, respectively. The overall effect of the action of the PFGs can be written as follows:

for ^{13}CH

$$A_1 = \frac{1}{2}\cos\left[\pi(\gamma_H + \gamma_C)g_1\delta + \pi\gamma_H g_2\delta\right],$$

for $^{13}CH_2$

$$A_2 = \frac{1}{2}\cos\left[\pi(2\gamma_H + \gamma_C)g_1\delta + \pi\gamma_H g_2\delta\right],$$

and for $^{13}CH_3$

$$A_3 = \frac{3}{8}\cos\left[\pi(3\gamma_H + \gamma_C)g_1\delta + \pi\gamma_H g_2\delta\right] + \frac{1}{8}\cos\left[\pi(\gamma_H + \gamma_C)g_1\delta + \pi\gamma_H g_2\delta\right],$$

where g and δ are the gradient strength and duration of the PFG pulse, respectively. The first gradient pulse usually causes a phase shift proportional to the quantum order $(n\gamma_H + \gamma_C)$, where n is the number of attached protons in the $^{13}CH_n$ groups. The effect of the first gradient pulse can be compensated by the second gradient pulse. By choosing an appropriate strength for the second gradient it is possible to selectively detect individual spin systems. When the same gradient shape and duration are used, the gradient strengths must be as follows:

for ^{13}CH

$$g_2 : g_1 = (\gamma_H + \gamma_C) : \gamma_H = -5 : 4, \qquad (8)$$

for $^{13}CH_2$

$$g_2 : g_1 = (2\gamma_H + \gamma_C) : \gamma_H = -9 : 4,$$

and for $^{13}CH_3$

$$g_2 : g_1 = (3\gamma_H + \gamma_C) : \gamma_H = -13 : 4.$$

Selective detection using PFG is accompanied by a 50% decrease in signal intensity. Moreover, any molecular self-diffusion processes can cause a signal attenuation on the multiple-quantum coherence, which is proportional to the square of the quantum order.[51]

The application of the MAXY method can be useful in the case of complex NMR spectra, *e.g.*, those of peptides or proteins, or biological fluids and tissue extracts. A general problem in the NMR studies of such objects is the overlap of signals (often, even if a very high magnetic field strength was used). Generally, the assignment of most spectral lines requires an extensive use of 2D NMR spectroscopy methods.[7] As an initial stage in the line assignment procedure before carrying out time-consuming 2D NMR experiments, it is useful to determine which lines correspond to ^{13}CH, $^{13}CH_2$ and $^{13}CH_3$ groups. The NMR spectra can be essentially simplified by suppression of water signals. This approach facilitates both signal assignment and structural studies of complex molecules.

3. MAXY-Based selective 2D NMR methods

Two-dimensional correlation NMR spectroscopy is a modern method used for signal assignment in the NMR spectra. It is based on a general approach in which the magnetisation is transferred from one spin to another through spin–spin coupling, chemical exchange or cross-relaxation. In the case of $^1H-^1H$ correlations, especially for macromolecules, signal overlap can present a serious problem and thus limit the application of the technique. A possible solution to such problem is to use the editing capabilities of the RELAY,[23,24] INEPT [25,26] and DEPT [27–29] methods in the experiments on heteronuclear correlation [36,41,46,48,52] and homonuclear correlation.[34,37–39,44–47] Signal overlap can be reduced owing to multiplicity selection and enhanced resolution of the 2D NMR spectra.

2D MAXY-Based pulse sequences are shown in Fig. 10.[44] In the time axis, the increment time (t_1) is placed at the centre, at the position where the $^{13}CH_n$ spin systems are in their highest quantum states. The 180° (^{13}C) pulse in the middle of the evolution period interchanges the quantum order and refocusses the ^{13}C chemical shift evolution in such a way that only ^1H chemical shifts have single-quantum coherence (SQ) for ^{13}CH, pure double-quantum coherence (DQ) for $^{13}CH_2$ and both triple-quantum (TQ) and single-quantum coherences for $^{13}CH_3$ groups.

A composite 180° (^{13}C) pulse can be utilised for suppression of undesired resonances in the ^{13}C spectral region, especially in the case of molecules containing aromatic and aliphatic carbon atoms. Thus, at the end of period t_1, the intensities of observable signals will be proportional to:[44]

$$-2\,I_x S_y \cos(2\pi\delta t_1)\Pi\cos(\pi J_j t_1)$$

for ^{13}CH,

$$-4\,I_x I_y S_x \cos(4\pi\delta t_1)\Pi\cos 2(\pi J_j t_1)$$

for $^{13}CH_2$, and

$$+2\,I_x I_y I_y S_y\left[3\cos(6\pi\delta t_1)+\cos(2\pi\delta t_1)\right]\Pi\cos^3(\pi J_j t_1) \text{ for } ^{13}CH_3.$$

Here δ represents the proton chemical shifts, J_j is the jth spin–spin coupling constant and $\Pi\cos(\pi J_j t_1)$ represents passive $^1H-^1H$ couplings evolving during t_1. It should be noted that the precession frequency of the $^{13}CH_n$ groups is proportional to the number, n, of the attached protons. Selective detection of the subspectra of the individual $^{13}CH_n$ groups can be achieved using the same technique as that used in the 1D experiments. Moreover, with a suitable acquisition mode, such as TPPI (Time-proportional Phase Incrementation),[51] it is possible to separate resonances from different $^{13}CH_n$ groups.[44]

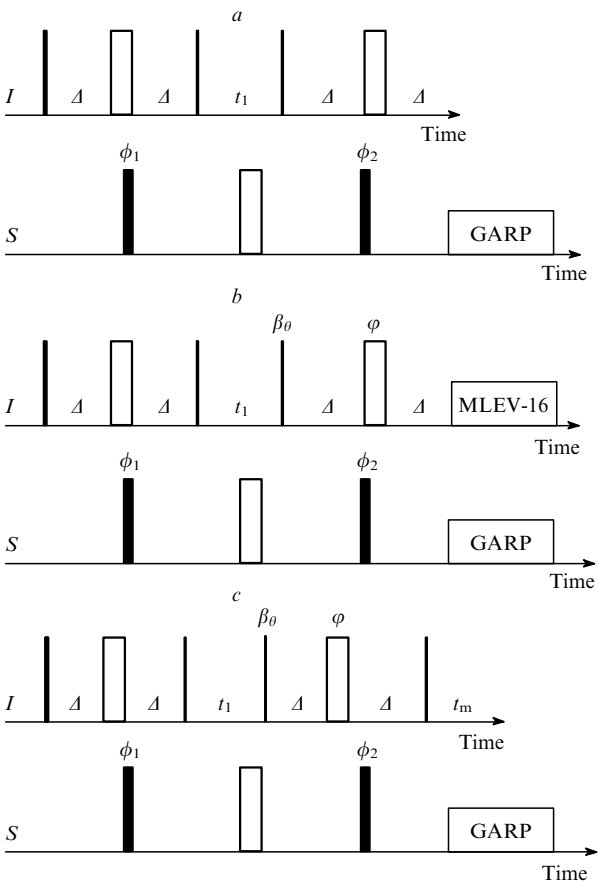


Figure 10. Pulse sequences based on 2D MAXY.
2D MAXY–COSY (Correlation Spectroscopy) (*a*), 2D MAXY–TOCSY (Total Correlation Spectroscopy) (*b*) and 2D MAXY–NOESY (Nuclear Overhauser Effect and Exchange Spectroscopy) (*c*).
MLEV-16 stands for M Levitt's Composite pulse Decoupling Sequence; t_1 is the increment time and t_m is the mixing time.

Coherence separation using TPPI. The TPPI method is widely used in phase-sensitive 2D experiments to achieve quadrature detection in the F_1 dimension.[51] In the 2D MAXY experiments, TPPI acquisition is achieved by increasing the phase of the mixing pulses 90°ϕ (^1H) and 180°φ (^1H) with an increment of 90° and 45°, respectively, starting from 0° for the non-selective experiment. The increase in the mixing pulse phase by 90° shifts the phase by −90° for SQ, by −180° for DQ and by −270° (+90°) for TQ, which is equivalent to the carrier frequency change [4] for the corresponding coherence. Thus, any quantum coherence can be separated and labelled by its carrier frequency or the number of protons in the $^{13}CH_n$ groups. These changes can be seen after each phase increment (Table 4).

The 90° increment of the phase $2\pi\delta t_1$ causes the functions $\cos(2\pi\delta t_1)$ and $\sin(2\pi\delta t_1)$ of the ^1H single-quantum and triple-quantum coherences to be observed in alternating experiments with different sign cycling (+ + − − for SQ and + − − + for TQ) corresponding to the −90° and +90° phase changes. Those of homonuclear double-quantum coherences of the $^{13}CH_2$ systems are always $\cos(2\pi\delta t_1)$ terms with the signs (+ − + −) because of the 180° phase change in frequency. The signals of the ^1H protons not attached to ^{13}C are unaffected by the TPPI scheme. After appropriate Fourier transformation, the single-quantum coherence peaks of ^{13}CH and $^{13}CH_3$ groups appear along a 45° diagonal and the triple-quantum signals appear along a −71.56° line in the F_1 dimension. The peaks corresponding to the double-quantum and zero-quantum coherences appear at

$$\omega' = |\omega_1 + \omega_2|,$$

Table 4. Change in the quantum coherence on phase change.

Spin system	Phase 0°	Phase 90°	Phase 180°	Phase 270°
^{13}CH	$+I_y\cos(2\pi\delta t_1)$	$+I_y\sin(2\pi\delta t_1)$	$-I_y\cos(2\pi\delta t_1)$	$-I_y\sin(2\pi\delta t_1)$
$^{13}CH_2$	$+(I_{1y}+I_{2y})\cos[2\pi(\delta_1+\delta_2)t_1]$	$-(I_{1y}+I_{2y})\cos[2\pi(\delta_1+\delta_2)t_1]$	$+(I_{1y}+I_{2y})\cos[2\pi(\delta_1+\delta_2)t_1]$	$-(I_{1y}+I_{2y})\cos[2\pi(\delta_1+\delta_2)t_1]$
$^{13}CH_3$	$+(9/4)I_y\cos(6\pi\delta t_1)$	$-(9/4)I_y\sin(6\pi\delta t_1)$	$-(9/4)I_y\cos(6\pi\delta t_1)$	$+(9/4)I_y\sin(6\pi\delta t_1)$
	$+(3/4)I_y\cos(2\pi\delta t_1)$	$+(3/4)I_y\sin(2\pi\delta t_1)$	$-(3/4)I_y\cos(2\pi\delta t_1)$	$-(3/4)I_y\sin(2\pi\delta t_1)$

(ω_1 and ω_2 are the chemical shift frequencies of the single-quantum coherences) with respect to the carrier frequency at the highest and lowest positions in the F_1 spectral window. Therefore, the complete spectrum is divided into four parts in the F_1 dimension. The upper part is the DQ COSY-spectrum of $^{13}CH_2$ protons, the middle part is the COSY-spectrum of ^{13}CH and $^{13}CH_3$ protons and the lower part is the TQ COSY-spectrum of $^{13}CH_3$ protons and any unsuppressed resonances of XH_n ($X \neq {}^{13}C$) groups (*ZQ*-spectrum) lying along the bottom line in the F_1 dimension. The positions of $^{13}CH_2$ and XH_n signals can be exchanged by decreasing the phase of the $90^\circ_\phi(^1H)$ pulse and increasing the phase of the $180^\circ_\varphi(^1H)$ pulse with 45° and 90° increments, respectively. Generally, this leads to an increase in the observable signal in proportion to $I_y\cos(m\pi)\cos(n2\pi\delta t_1 - nm\pi/2)$, where m is the number of phase increments. For selective measurements, the TPPI scheme can be applied to the $90^\circ_\phi(^1H)$ and $180^\circ_\varphi(^1H)$ pulses with phase increments of $90^\circ/n$ and $90^\circ/2n$, respectively.

MAXY – TOCSY. The magnetisation transfer from a spin (I_i) to its coupling partners I_j can be achieved by the homonuclear Hartmann – Hahn mechanism.[51, 53–58] This can be done with ease by adding a TOCSY magnetisation transfer step before the data acquisition.[44]

MAXY – NOESY. When a $90^\circ_x(^1H) - t_m - 90^\circ_x(^1H)$ scheme is inserted before data acquisition, it is possible to obtain cross-peaks due to nuclear Overhauser effect (NOE) or chemical exchange.[44] For a $^{12}C-{}^1H_A-{}^{13}C-{}^1H_B$ spin system, the first pulse will convert the coherence to longitudinal magnetisation as I_{zB} and $I_{zA}\cos(\omega t_1)$, respectively. The NOE magnetisation transfer occurs during the mixing of different states of the coupled spin system. The final $90^\circ_x(^1H)$ pulse re-establishes the single-quantum coherence of spin *I*. The observed NOE cross-peak corresponding to coherence transfer from the H_B proton to the H_A proton is defined as

$$I_A = I\cos(\omega_B t_1)\frac{\sigma_{AB}}{(\lambda_1-\lambda_2)[\exp(-\lambda_1 t_m)-\exp(-\lambda_2 t_m)]}\Bigg\},$$

where $\lambda_{1,2} = (1/2)\{(R_A+R_B) \pm [(R_A-R_B)^2+4\sigma_{AB}\sigma_{BA}]^{1/2}\}$, σ_{AB} and σ_{BA} are the cross-relaxation rates from spin A to spin B (AB) and from spin B to spin A (BA), respectively, R is the longitudinal relaxation rate including all terms except for the cross-relaxation rate σ_{AB}. To calculate the maximum possible NOE, one must differentiate this equation with respect to t_m. Suppose that

$$R_A = R_B = 2\sigma_{AB} = 2\sigma_{BA},$$

$$\lambda_1 = 3\sigma,$$

$$\lambda_2 = \sigma.$$

Then one gets

$$t_m(\max) = \frac{\ln 3}{2\sigma} \approx 1.1T_1.$$

If

$$\frac{\sigma_{AB}}{\lambda_1-\lambda_2} = 0.5,$$

the maximum NOE enhancement is

$$I_{cross}(\max) = -0.19\, I_{zB}(t_1).$$

The MAXY – TOCSY and MAXY – NOESY spectra can provide information on the type of the spin system provided that two spins are involved in a dipole – dipole coupling.

4. Selective *J*-resolved 1D NMR spectroscopy. MAXY – JRES

Using *J*-resolved NMR spectroscopy, it is possible to separate the chemical shifts and the spin – spin coupling constants into the F_1 and F_2 dimensions, respectively,[3, 59] and thus obtain a broadband-decoupled 1D NMR spectrum from the projection on the F_2 dimension. However, for complex samples (*e.g.*, biological fluids [60, 61]), the method is of limited use because of strong overlap of NMR resonances. Procedures used for spectral resolution enhancement and lineshape improvement include pseudo-echo-weighting,[62] 'time-reversal'[63] and other techniques,[64, 65] specific data processing[65, 66] and the 3D JRES – COSY NMR spectroscopy[67, 68] (here, JRES stands for J Relay Selective). The MAXY approach can be successfully employed for obtaining individual JRES-spectra of ^{13}CH, $^{13}CH_2$ and $^{13}CH_3$ groups.[45] The MAXY – JRES pulse sequence is shown in Fig. 11. An advantage of the MAXY technique is the possibility of using magnetic field gradient pulses for separation of the subspectra of CH_n groups. The gradient strength ratios, $g1:g2:g3:g4$, are as follows:

Nonselective spectrum	$^{13}CH + {}^{13}CH_3$	^{13}CH	$^{13}CH_2$	$^{13}CH_3$
1:1:4:5	1:(−1):2:4	1:(−1):2:4	1:(−1):2:6	1:(−1):2:8

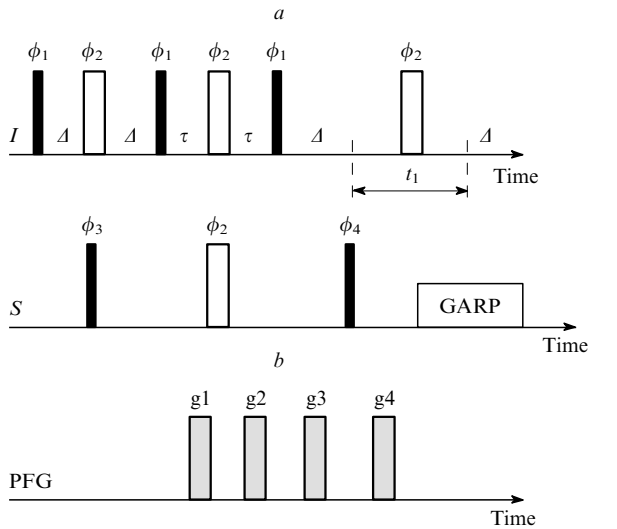


Figure 11. The RF pulse sequence (*a*) and PFG sequence (*b*) in the MAXY – JRES experiments.
The delay Δ is $1/(2\,{}^1J_{CH})$; τ is the short delay for compensation of the pulse phase, t_1 is the increase in the magnetisation evolution time. The pulse phase cycling scheme is as follows: $\phi_1 = 0^\circ$; $\phi_2 = 90^\circ$; $\phi_3 = 0^\circ$, 180°; $\phi_4 = 0^\circ$, 0°, 180°, 180°.

The selective spectrum of a $^{13}CH_n$ group can also be obtained using the phase cycling scheme.

5. 2D correlation NMR spectroscopy of geminal protons

Using a 2D method, which shows correlations only between geminal protons of methylene groups, it is possible to simplify both a COSY spectrum and signal assignment.[37, 38, 44, 47] Two pulse sequences were reported,[37] named gem-COSY – MQ (Fig. 12 *a*) and gem-COSY – PT (Fig. 12 *b*) and based on the inverse-DEPT-90 (see Ref. 31) and inverse-INEPT-1/(2^1J_{CH}) (see Ref. 33) techniques, respectively. The techniques were modified in such a fashion that the H → ^{13}C → H magnetisation transfer was restricted to one-bond couplings. For a spin system $I_1 - S - I_2$, the initial 90° (I) excitation pulse creates negative magnetisation along the y-axis of the I_1 spin ($-I_{1y}$) in both pulse sequences.[37] After the evolution and mixing periods, the expressions for the observable signals are as follows:

gem-COSY – MQ

$$\sigma = -I_{2y}\cos(2\pi\delta_1 t_1)\cos(\pi J_{12} t_1)\Pi\cos(\pi J_{1j} t_1) + 2\, I_{1x}I_{2z}\cos(2\pi\delta_1 t_1)\sin(\pi J_{12} t_1)\Pi\cos(\pi J_{1j} t_1), \quad (9)$$

gem-COSY – PT

$$\sigma = -I_{2x}\cos(2\pi\delta_1 t_1)\cos(\pi J_{12} t_1)\Pi\cos(\pi J_{1j} t_1) - 2I_{1z}I_{2y}\cos(2\pi\delta_1 t_1)\sin(\pi J_{12} t_1)\Pi\cos(\pi J_{1j} t_1) \quad (10)$$

(σ is the density operator). Equation (10) describes the double magnetisation transfer $I_1 \to S \to I_2$, which gives rise to a cross-peak equivalent to an analogous peak in the COSY spectrum, except that it has an in-phase doublet pattern (J_{12}) in both frequency dimensions. Equation (10) describes the magnetisation back-transfer $I_1 \to S \to I_1$, which gives rise to a double diagonal dispersion peak with antiphase splitting (J_{12}). Passive ^{1}H – ^{1}H coupling described by the term $\Pi\cos(\pi J_{1j} t_1)$ has the same meaning as in conventional correlation spectroscopy.[37] An alternative method of obtaining gem-COSY spectra involves modification of the 2D MAXY pulse sequence (Fig. 12 *c*).[44, 47] If a $90^\circ_x(^1H) - \Delta - 90^\circ_x(^{13}C)180^\circ_x(^1H) - \Delta - 90^\circ_y(^1H)$ is used, the $^{13}CH_n$ spin systems will be excited to the second maximum possible quantum order (n for $^{13}CH_n$ or $n-1$ for ^{1}H) as shown below:

for ^{13}CH

$$I_z \longrightarrow +2\, I_z S_y \text{ (SQ)},$$

for $^{13}CH_2$

$$I_{1z} \longrightarrow -4\, I_{1z}I_{2x}S_x \text{ (DQ)},$$

for $^{13}CH_3$

$$I_z \longrightarrow -8 I_x I_x I_z S_y \text{ (TQ)}.$$

The modification of the MAXY pulse sequence is that the second 90°(^{1}H) pulse is applied along the y axis; therefore, the spin-I_1 coherence is transferred to I_2 during the preparation period. At the end of the coherence evolution time, we get:

for ^{13}CH (SQ)

$$+2\, I_z S_y,$$

for $^{13}CH_2$ (DQ)

$$4\, I_{1z}I_{2y}S_x\cos(2\pi\delta_2 t_1)\cos(\pi J_{12} t_1)\cdot \Pi\cos(\pi J_{1j} t_1 + 2\, I_{2y}S_x\cos(2\pi\delta_2 t_1)\sin(\pi J_{12} t_1),$$

for $^{13}CH_3$ (TQ)

$$-8\, I_y I_y I_z S_y \sin^2(2\pi\delta t_1)\Pi\cos^2(\pi J_j t_1).$$

After the mixing scheme $90^\circ_x(^1H) - \Delta - 90^\circ_x(^{13}C) - 180^\circ_x(^1H) - \Delta$, the observable single-quantum coherence is:

$+I_y$ for ^{13}CH,

$+I_{1y}\cos(2\pi\delta_2 t_1)\cos(\pi J_{12} t_1)\Pi\cos(\pi J_{1j} t_1) - 2\, I_z I_{2x}\cos(2\pi\delta_2 t_1)\sin(\pi J_{12} t_1)$ for $^{13}CH_2$

and

$-(1/2)\, I_y[\cos(4\pi\delta t_1) + 1]\Pi\cos^2(\pi J_j t_1)$ for $^{13}CH_3$.

Signals of ^{13}CH groups appear in the zero-frequency region along the bottom line in the F_1 dimension and signals of a $^{13}CH_3$ group will appear as two peaks corresponding to double-quantum and zero-quantum coherences with the same initial intensity in the F_1 dimension. For $^{13}CH_2$ groups, the first term describes the $I_1 \to I_2S(t_1) \to I_1(t_2)$ transfer, which gives rise to a cross-peak equivalent to that in a conventional COSY spectrum with the exception that multiplets are in-phase in both measurements. The second term describes the $I_1 \to I_2S(t_1) \to I_2(t_2)$ transfer responsible for the appearance of diagonal peaks with dispersion doublet lineshapes. If the phase of the last 90°(^{1}H) pulse alternates about the x axis, the sign of the CH_2 cross-peak is the same, whereas the signs of the peaks of other groups are altered. This offers yet another way of obtaining diagonal peak suppressed gem-COSY spectra, as in the 2D MAXY NMR spectrum.

The TOCSY and NOESY transfers can also be used in the gem-COSY experiments. The MAXY method provides a better suppression of diagonal peaks compared to the original MQ method. Proton signals of ^{13}CH, $^{13}CH_2$ and $^{13}CH_3$ groups are observed separately in different parts of the spectrum. $^{13}CH_2$ group protons give a normal gem-COSY spectrum. $^{13}CH_3$ proton signals appear at the right lower region of the spectrum. ^{13}CH proton peaks are along the bottom line of the spectrum together with zero-quantum coherence correlation of $^{13}CH_3$ protons. 2D correlation NMR spectroscopy of geminal protons appeared to be useful for analysis of the spectra of large molecules[47] and provides an alternative method of editing ^{1}H NMR spectra.

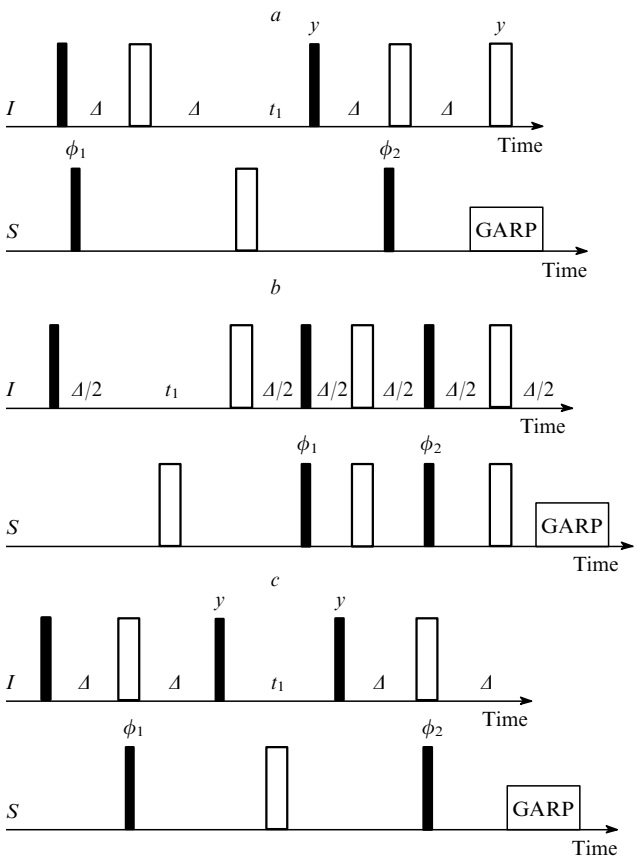


Figure 12. gem-COSY – MQ (*a*), gem-COSY – PT (Polarisation Transfer) (*b*) and gem-COSY (*c*) pulse sequences based on the MAXY sequence.

6. Spin–spin coupling constants measurement using MAXY-based experiments

The spin–spin coupling constant is one of the most important parameters in NMR spectroscopy and has been widely used in conformational analysis of complex molecules and in structural modelling.[2,4,69–74]

For the first-order spectra of symmetrical systems the spin–spin coupling constants can be measured directly in the NMR spectrum. However, in the case of complex molecules, line assignment is very difficult because of signal overlap.

Using the MAXY method, it is possible to obtain 2D NMR subspectra of individual $^{13}CH_n$ groups or separate the spectra into different spectral regions according to the number, n, of the protons bonded to ^{13}C, thus resulting in appreciable reduction of signal overlap. For instance, the 2D MAXY technique was used to determine the spin–spin coupling constants in the neurotensin molecule.[75] Although neurotensin is a relatively short peptide, proton signals in its ^1H NMR spectrum are strongly overlapped, especially in the low-frequency region. The use of the 2D MAXY method with correlation of only $^{13}CH_2$ groups permits resolution enhancement of most overlapped peaks including the β-proton peaks.

V. Measurements of self-diffusion coefficients

At present, self-diffusion coefficients are very often measured using the pulsed magnetic field gradient technique according to Stejskal and Tanner.[76]

Once the Longitudinal Eddy Current Delay (LED) pulse sequence was designed and the concept of diffusion-ordered spectroscopy proposed, it became possible to determine the diffusion coefficients associated with each resonance signal in the high-resolution NMR spectrum. Therefore, researchers expressed increased interest in measuring diffusion coefficients using NMR spectroscopy.[77–87] The diffusion coefficients thus determined were used in, *e.g.*, experimental studies on the vesicle size distribution in phospholipids,[82] molecular mass distribution in polymers,[83] in analysing complex mixtures of cell extracts,[85] protein association,[86] aggregation of insulin molecules[87] and protein binding with drugs.[88–107] Editing 1D and 2D NMR spectra of biological fluids, based on differences in the molecular diffusion coefficients and relaxation times, is possible using the DIRE (Diffusion Relaxation) and DETOCSY (Delay TOCSY) techniques[108] and improved 2D methods of the HETCOR (Heteronuclear Correlation Spectroscopy), COSY and NOESY types.[109–111]

In an original PFG–SE (Pulsed Field Gradient Spin Echo) experiment, signal attenuation can be written as follows[76]

$$\ln\frac{A(g)}{A(0)} = -\gamma^2 D\left[\frac{2g_0^2\tau^3}{3} + gg_0\delta\left(\frac{3\tau^2}{2} - \frac{\delta^2}{6}\right) + g^2\delta^2\left(\Delta - \frac{\delta}{3}\right)\right] - \frac{2\tau}{T_2}. \quad (11)$$

Here $A(g)$ and $A(0)$ are the signal intensities in the presence and in the absence of PFG, γ is the magnetogyric ratio for a given spin, D is the diffusion coefficient, g_0 is the steady magnetic field gradient, g and δ are the strength and duration of the rectangular gradient pulse, Δ is the time interval between the starting points of two gradient pulses (diffusion time), 2τ is the time at which spin echo occurs and T_2 is the transverse relaxation time. If

$$g_0^2 = \tau^3 \ll g^2\delta^2\Delta,$$

Eqn (11) is simplified

$$\ln\frac{A(g)}{A(0)} = -\gamma^2 Dg^2\delta^2\left(\Delta - \frac{\delta}{3}\right) - \frac{2\tau}{T_2}. \quad (12)$$

This equation is known as the Stejskal–Tanner equation for diffusion coefficient measurement.

Having obtained a number of spectra using different gradient strengths and plotted $\ln A$ *vs.* $\gamma^2g^2\delta^2(\Delta-\delta/3)$, one gets a straight line with the slope equal to the self-diffusion coefficient. In order to determine the exact D values, one must attenuate the NMR signal. This can be achieved using a wide range of gradient pulses. For slowly diffusing particles the gradient strength can be of the order of 1000 to 2000 mT m^{-1}.

Alternating eddy flows that can be induced in a sample under study in the course of experiments complicate exact detection of the NMR signal.[112] It is also possible to obtain the same range of $\gamma^2g^2\delta^2(\Delta-\delta/3)$ values using small gradients with compensation of alternating eddy flows owing to longer diffusion time.[113,114] However, this can lead to a decrease in sensitivity due to spin relaxation.[113]

Another way of increasing gradient strength is to use the dependence of the dephasing/rephasing of gradient pulses on the quantum order of the spin systems affected[115] by the gradients during the multiple-quantum sequence. In this case the effective magnetogyric ratio γ_{ef} is the sum of the values, γ, of the spins involved in coherence. For a homonuclear double-quantum sequence one has $\gamma_{ef} = 2\gamma$; therefore, the gradient strength is doubled while the measurable diffusion coefficient decreases by a factor of four.[116–120] Diffusion spread of longitudinal spin orders $2I_zI_z$ and $4I_zI_zI_z$ normal to the gradient direction was studied.[118,119] It was shown that the effective magnetogyric ratios are equal to 2γ and 0 for the $2I_zI_z$ system and to 3γ and γ for the $4I_zI_zI_z$ system.

The MAXY method was modified[43–46,121–123] to determine diffusion-induced changes in the maximum quantum order of the spin operator $8I_xI_yI_yS_y$ for the $^{13}C^1H_3$ (SI_3) spin system. This system is characterised by four magnetogyric ratios, namely, $(3\gamma_H+\gamma_C)$, $(3\gamma_H-\gamma_C)$, $(\gamma_H+\gamma_C)$ and $(\gamma_H-\gamma_C)$, corresponding to four multiple-quantum levels composed of possible combinations of individual spin states. The multiple-quantum coherences (each of them can be obtained individually using pulsed field gradients) can be converted to observable single-quantum coherences. Diffusion-induced changes in each coherence can also be measured individually.[43–46]

An original technique[124] permits reduction of the duration of the 3D NMR experiments; the corresponding pulse sequence is given in Fig. 13. The modification of the MAXY sequence consists of addition of a diffusion time and diffusion gradient

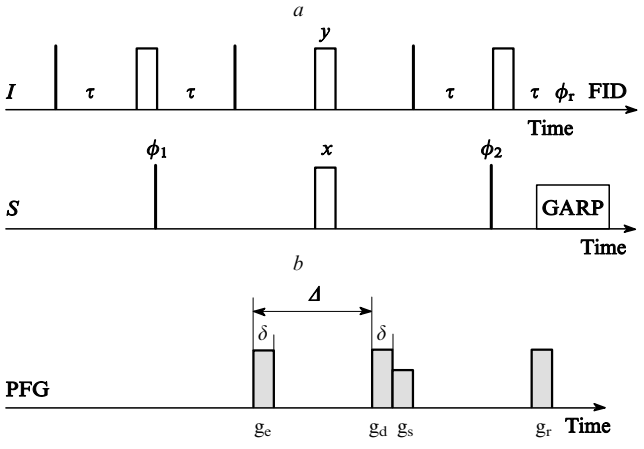


Figure 13. The RF pulse sequence (*a*) and PFG sequence (*b*) used in the modified MAXY diffusion coefficient measurement technique.
The pulse phases in the rotating frame are along the x axis until otherwise specified, *i.e.*, $\phi_1 = x, -x$; $\phi_2 = x, x, -x, -x$; $\phi_r = -y, y, y, -y$. The delay time τ is 3.85 ms, the time interval Δ is set to 50 ms; FID stands for Free Induction Decay. For notations g_e, g_d, g_s and g_r, see text.

pulses (encoding gradient g_e and decoding gradient g_d). The coherence-selective and read pulse strengths (g_s and g_r, respectively) are chosen according to the desired quantum order and fixed. The interval τ is set to $1/(2\,{}^1J_{SI})$; this delay period is too short for significant homonuclear J precession to occur.[125]

This pulse sequence was used in the diffusion coefficient measurements in studies of D,L-alanine.[126]

Most diffusion coefficient measurement techniques[127] are comparatively time-consuming because they include either a series of NMR experiments or a 2D DOSY (Diffusion-Order Spectroscopy) experiment. A 1D DOSY method[128] for the determination of diffusion coefficients in a single experiment (scan) involves spatial variation of the parameters of a conventional STE (Stimulated Echo) pulse sequence[78] in such a manner that all the scans necessary for the determination of diffusion coefficient could be performed simultaneously in different regions of the sample. The spectrum is recorded in the presence of a weak read gradient and therefore the lineshape contains the necessary information. For well-resolved spectra with high signal-to-noise ratio the method allows the duration of the experiment to be shortened by an order of magnitude (to 1 s), which is important in studies of those samples whose state rapidly changes with time.

Diffusion, relaxation and the spin–spin coupling precession directly affect the accuracy of measurements of coefficients. The larger the Δ value, the smaller the gradient strength or duration; however, signal attenuation due to transverse relaxation $\exp(-\Delta/T_2^*)$ leads to a decrease in the signal-to-noise ratio. To compensate for the loss of sensitivity, it is necessary to obtain a larger number of spectra, which increases the duration of the experiment.

Thus, methods based on the MAXY sequence can be successfully implemented on spectrometers with low gradient strength and low magnetic field for measuring small diffusion coefficients (in macromolecules and molecular ensembles). Signal attenuation due to self-diffusion can be observed simultaneously for all coherences using 2D NMR spectroscopy or for a certain coherence using magnetic field gradient pulses. In the case of systems with natural abundance of ^{13}C the sensitivity of such methods is low. However, they can be suitable for measuring the diffusion coefficients of ^{13}C-labelled molecules in complex mixtures such as biological fluids or cell extracts.

Now consider again Eqn (11). If the condition $g_0^2\tau^3 \ll g^2\delta^2\Delta$ is not met, the effect of the steady gradient must be accounted for. There are two factors that have a negative effect on the accuracy of measurements; these are the steady gradient and thermal convection. The steady gradient is due to inhomogeneity of the static magnetic field in the sample, which can be eliminated using the spin echo technique.[88–90] This approach is widely used in transverse relaxation time measurements. Thermal convection particularly manifests itself if experiments are carried out at high temperatures.

To obtain reliable values of metabolite diffusion coefficients in biological fluids, the diffusion coefficients must be measured at physiological temperature.[80,81] Since in most NMR spectrometers the temperature is maintained with an upstream gas (nitrogen or air) flow, a temperature gradient is created in the sample, which is responsible for the onset of convection flow. In addition, time-dependent temperature gradients are created when the gradient pulses are switched on and off.

Problems associated with convection were analysed by Carr and Purcell[91] in the early studies of the spin echo effect and diffusion. In the multiple spin-echo gradient experiments carried out in the presence of convection flows the amplitudes of the even echo signals are larger than those of the odd signals. This is due to the fact that the effect of thermal convection during the odd echo is compensated for during the even echo. Therefore, the simplest method is to measure only the even echo signals. This approach was implemented in the PFG–STE method and its versions involving doubling of the pulse sequence.[93,94] It should be noted that the diffusion gradients in the PFG–STE pulse sequence and its versions, such as LED, act for coherence selection, as in gradient enhanced NMR spectroscopy.

The use of coherence-selective gradients causes the sensitivity of the method to be halved. Doubling the STE and LED sequences again halves the sensitivity so it totally decreases by a factor of four. This is equivalent to shortening of the transverse relaxation

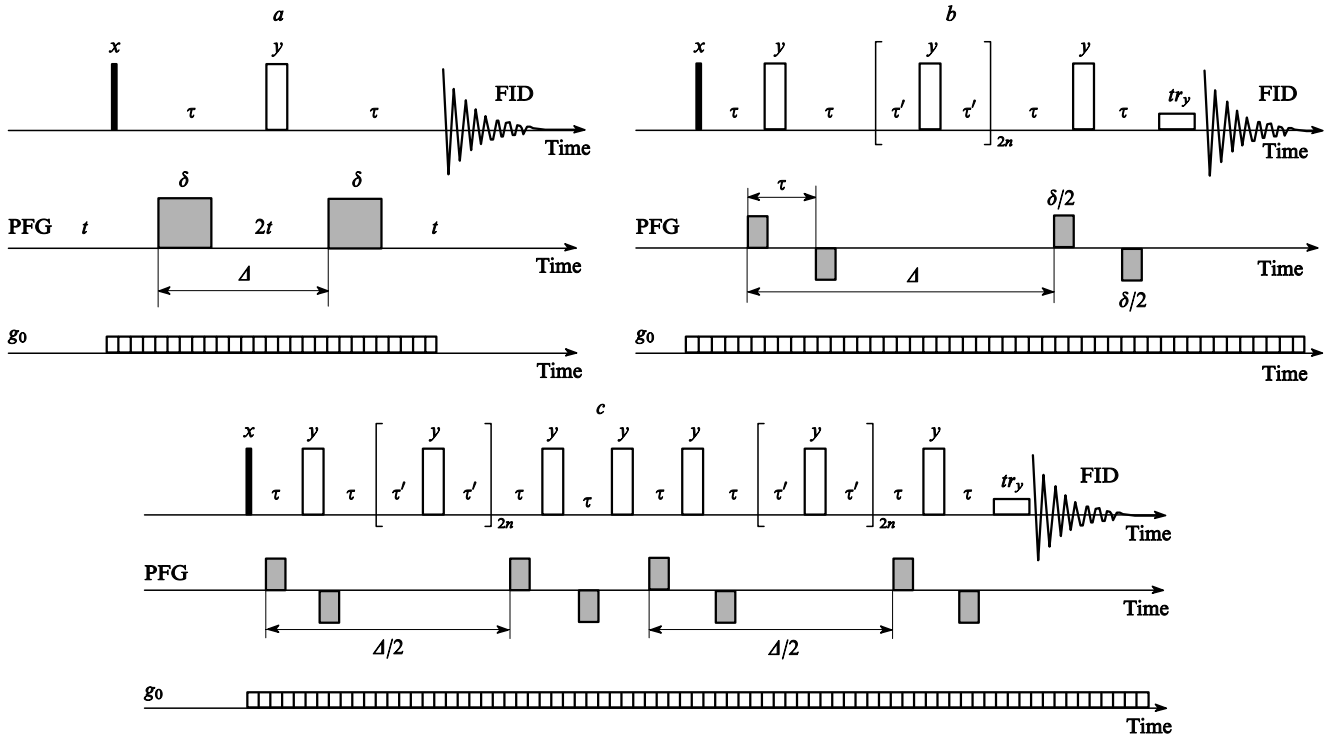


Figure 14. The RF pulse sequences and the PFG sequences used in the spin-echo (SE) methods for diffusion coefficient measurements (*a*), MSE (Multiple So) (*b*) and DMSE (*c*).

time by a factor of $1.4\,T_2$. The T_2 times of metabolite spins in biological fluids lie between a few hundreds of milliseconds and a few seconds; therefore, one can expect that a compensation technique based on the double PFG–SE sequence for diffusion times shorter than T_2 will be more sensitive than the coherence transfer method.

In the Carr–Purcell–Meiboom–Gill (CPMG) method [97,98] the spin echo is used for T_2 measurements at a spin stabilisation time of up to a few seconds under conditions of minimum phase distortions. Using this technique, it is possible to obtain a homogeneous static magnetic field (steady gradients) and compensate for artifacts that appear due to distortions of the 180° pulses. Based on the CPMG sequence, a pulse sequence was created for measuring diffusion coefficients in the presence of steady gradients and thermal convection (Fig. 14*a*). Bipolar pulses were used instead of the gradient pulse (Fig. 14*b*). In addition, a multiple spin-echo pulse sequence was implemented instead of a single 180° pulse, which permits operation with long diffusion times. The last pulse before data acquisition removes the dispersion component from the detected signal. This pulse scheme is doubled and therefore was named DMSE (Double Magnetic Spin Echo, Fig. 14*c*). To ensure bipolar gradient pulses, a 180° pulse is incorporated in the middle of the sequence. Theoretical description and the results of tests with human blood plasma and human seminal fluid were reported recently.[123] The results were compared with the data obtained using the BP–LED (Bipolarisation LED) [100] and MSE methods. The temperature of diffusion coefficients obtained using these three pulse sequences are shown in Fig. 15.

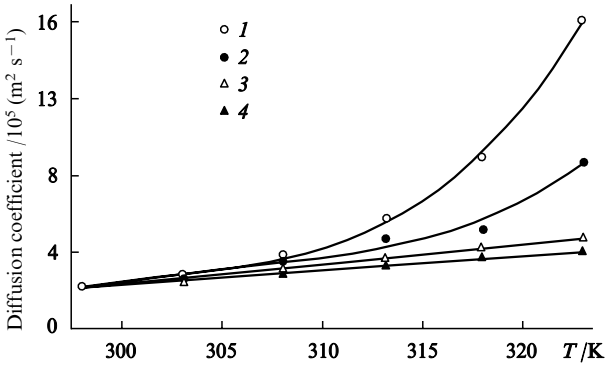


Figure 15. Temperature dependence of water diffusion coefficients measured using the BP–LED (*1*), MSE (*2*), DMSE (*3*) and other (*4*) methods in the range 298.2–323.2 K.

The DMSE technique permits efficient suppression of thermal convection,[123] being unaffected by the steady gradients. Incorporation of the CPMG sequence into the DMSE sequence allows one to operate with long diffusion times and suppress broad NMR peaks with short transverse relaxation time T_2. This possibility of spectral editing makes the DMSE technique suitable for studying the molecular mobility in complex systems. Among the other advantages of this method are good lineshapes and base line and efficient suppression of water signals.

VI. Observation of 'underwater' signals. RECUR NMR technique

Efficient suppression of water signals is of crucial importance in NMR spectroscopy of complex systems.[58] The main efficiency criteria are as follows:

— high degree of suppression of the water peak, which is five to six orders of magnitude more intense than the peaks of the molecules under study,

— high selectivity to the signals appearing near the water peak and

— short duration of the solvent signal suppression sequence in order to minimise the magnetisation transfer to the exchanging protons.

Among the methods designed to meet these criteria, the WET (Water Eliminated Transfer) [129] and WATERGATE (Water Gate) [130] techniques can be pointed out. The best, with respect to all criteria, is the modified WATERGATE method.[131] However, these schemes have a common drawback consisting of suppression of 'underwater' peaks.

Attempts at solving this problem in studies of macromolecules included taking into account the longitudinal relaxation time (T_1) difference between water and the macromolecule. This means that by choosing an appropriate recovery time, which follows the inversion scheme, it is possible to observe the signals of macromolecules.[132] T_1-Editing was performed using the heteronuclear multiple quantum coherence (HMQC) method modified by incorporating magnetic field gradients.[133] The approach is efficient in natural abundance ^{13}C or ^{15}N studies. If the repetition time of experiments is short, the water signal can be partly suppressed owing to longer relaxation time compared to the relaxation times of the macromolecule. HMQC, HSQC (Heteronuclear Single Quantum Coherence) and magnetic field gradient experiments give satisfactory results and there is no need for further suppression of water signals. However, a long pre-delay time is required in studies of small molecules and therefore both water signals and ^{12}CH signals must be additionally suppressed using the Bilinear Rotation Decoupling (BIRD) sequence. One can also use diffusion filtering for attenuation of the signals of diffusing water as in, *e.g.*, the DRYCLEAN (Dry Clean) technique.[134] However, these approaches are inapplicable in studies of small metabolite molecules in biological fluids due to similar T_1 values and diffusion coefficients for the molecules in question and water protons.

A number of methods based on the relaxation time T_2 differences between water signals and signals of the molecules under study are also used. They are particularly efficient if the relaxation time T_2 of the water signal can be reduced by, *e.g.*, adding paramagnetic impurities.[135]

Some techniques were designed in order to avoid difficulties that appear when the desired signal of proton A is masked by other proton signals and thus cannot be selectively excited. The key feature of these methods is selective excitation of the second proton B coupled to the desired proton A. The magnetisation is transferred from B and A using the COSY or TOCSY sequence and the second selective pulse excites the proton A (*e.g.*, NOE or ROE, or Rotating-frame Overhauser Effect). Using appropriate magnetic field gradient pulses, it is possible to eliminate undesired coherences in this scheme. Such methods [136–140] were named gs-1D CONO (COSY–NOESY), gs-1D TONO (TOCSY–NOESY) and gs-1D TORO [TOCSY–ROESY (Rotating-frame Overhauser Effect Spectroscopy)]. There are also the gs-1D ROTO and gs-1D RORO techniques which begin with the ROESY transfer. However, one should keep in mind that if a pulse sequence includes a number of selective pulses, long duration of these pulses can complicate experiments owing to long relaxation of useful signal.

A method of 'underwater' signal recovery using magnetisation transferred NMR spectroscopy, named RECUR NMR (Recovery of 'Underwater' Resonances NMR), was proposed.[138] The technique is based on a modified WATERGATE suppression scheme followed by magnetisation transfer. This method offers considerable advantages over other techniques.[136,139] Water signal suppression occurs involving a double WATERGATE sequence with a five-lobe composite pulse (W5), as shown in Fig. 16*a*.

The 'underwater' signals can be recovered using both the TOCSY and ROESY sequences which execute magnetisation back-transfer to the 'underwater' signals using scalar or dipole–dipole couplings, respectively, in 1D RECUR–TOCSY experiments (Fig. 16*b*). It should be noted that both coherence transfer

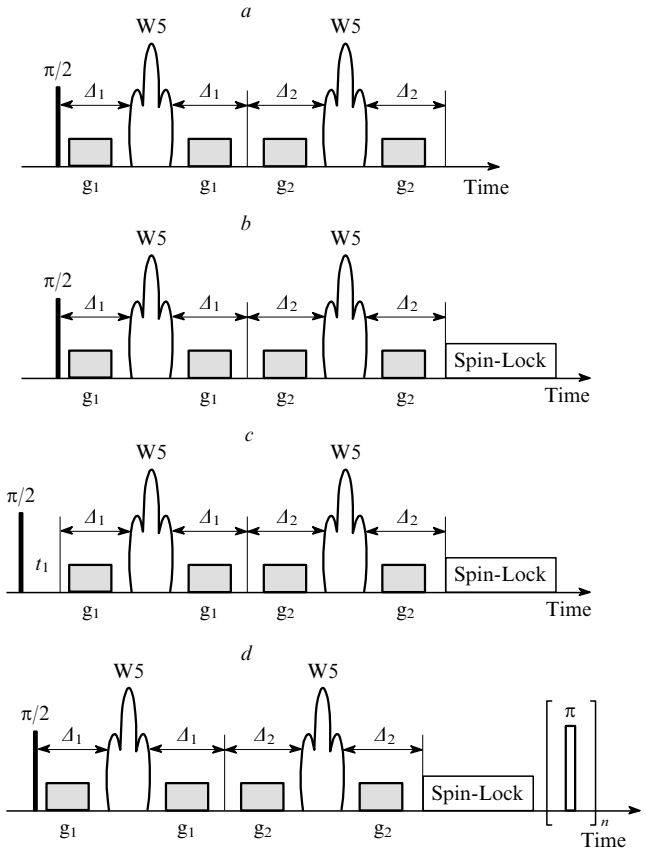


Figure 16. Conventional WATERGATE-W5 two-pulse sequence (*a*), 1D RECUR – TOCSY pulse sequence (*b*) and 2D RECUR – ROESY pulse sequence (*c*) containing the MLEV-17 spin stabilisation pulse sequence or a long pulse to create a TOCSY or ROESY type magnetisation transfer for recovery of 'underwater' signals; the RECUR – JRES and RECUR – CPMG pulse sequences (*d*).

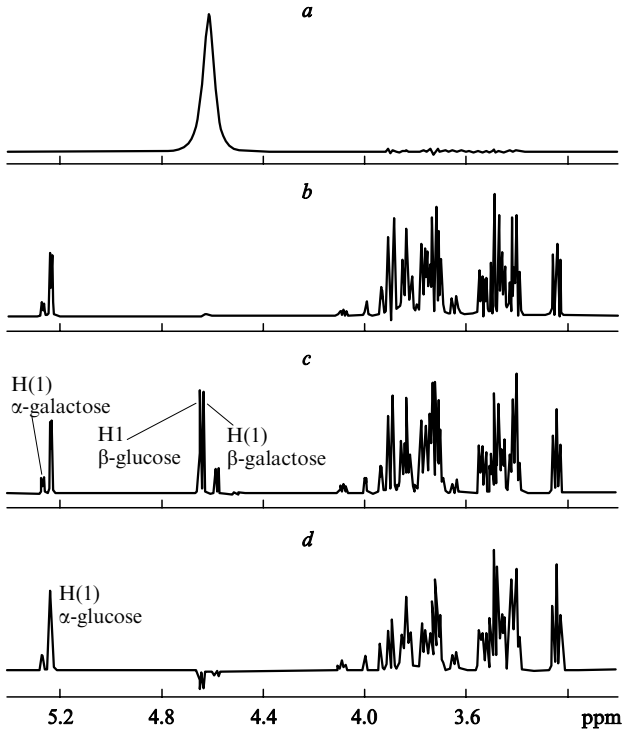


Figure 17. 1D NMR spectra of D-glucose and D-galactose obtained without (*a*) and with (*b*) water signal suppression using the WATERGATE double pulse sequence.
H(1) proton 'underwater' signals completely recovered using the RECUR – TOCSY (*c*) and RECUR – ROESY (*d*) methods.

schemes lead to in-phase magnetisation. This makes it possible to measure the ROE buildup rate in 1D NMR experiments using the pulse sequence shown in Fig. 16 *b* or in 2D NMR experiments (Fig. 16 *c*). By incorporating the CPMG sequence before the data acquisition step (see Fig. 16 *d*, RECUR – CPMG) one can measure the transverse relaxation times of any underwater resonance. If a single spin echo technique is employed instead of this scheme, the pulse sequence can be implemented in $^1H - ^1H$ homonuclear JRES NMR spectroscopy (RECUR – JRES).

The pulse sequence shown in Fig. 16 *c* differs from the WATERGATE – TOCSY and WATERGATE – ROESY [136, 139] sequences, in which the WATERGATE module follows the magnetisation transfer scheme. These methods involve suppression of 'underwater' signals and permit 2D NMR spectroscopy studies of macromolecules. But they cannot be implemented in 1D NMR spectroscopy experiments and prevent the ROE buildup rate or T_2 of the 'underwater' signals from being measured.

The RECUR method was tested [138] using a 4 : 1 model mixture of D-glucose (20 mg ml^{-1}) and D-galactose (5 mg ml^{-1}) in 1 : 1 $H_2O - D_2O$ solution. NMR spectra with and without water signal suppression, obtained using the double WATERGATE sequence, are shown in Fig. 17 *a*,*b*. After TOCSY (Fig. 17 *c*) or ROESY (Fig. 17 *d*) magnetisation transfer with mixing times of 80 ms and 1.5 s, respectively, the 'underwater' signals are completely recovered. TOCSY magnetisation transfer occurs more efficiently. However, in the absence or in the presence of a weak spin – spin coupling the RECUR – ROESY method is optimum.

At a sufficiently high concentration of the substance under study, NMR resonances of individual CH_n groups (*e.g*, CH_3) can be recovered using the MAXY sequence.[43, 44] The proton spin – spin relaxation times obtained using the RECUR – CPMG sequence are as follows:[138]

Compound	β-Glucose	β-Galactose	α-Glucose	α-Galactose
Time /s	1.1	1.5	1.3	1.3

The 2D RECUR – ROESY NMR technique was used in studies of a human blood plasma sample to determine the internuclear distance in the glucose molecule.[138]

The RECUR – TOCSY and ROESY methods can also be used for spectral editing. For instance, at a spin stabilisation time of 70 ms it is possible to observe signals of the most flexible structural fragments of lipoproteins. Extension of this time to 700 ms causes an appreciable weakening of these signals while the signals from small metabolite molecules become less suppressed owing to comparatively longer relaxation times. When analysing 2D JRES NMR spectra, this approach allows visualisation of all peaks from small molecules, including the 'underwater' signals. The TOCSY or ROESY techniques allow the T_2, internuclear ROE and ROE buildup rate to be measured, which is important in molecular structure and dynamics studies.

VII. Homonuclear selective methods

1. Selective COSY experiments

Combining selective and conventional 'hard' pulses in a single experiment permits design of a new approach, which can conveniently be exemplified by the COSY sequence.[141 – 143]

The pulse sequence shown in Fig. 18 was used in the study of brucine (Fig. 19). The coherence diagram shows that the selective 90° pulse creates coherences I^+ and I^-. The antiphase magnetisation, $2I_{H1y}I_{H2z}$, of proton 2 coupled to the first excited proton I_{H_1} evolves during the d2 delay time equal to (1/2)J(H,H). Then, a 'hard' 90° pulse p2 converts it to $2I_{H1z}I_{H2y}$. Thus, in the data acquisition step the phase magnetisations of all the brucine protons (see Fig. 19) coupled to the selectively excited proton

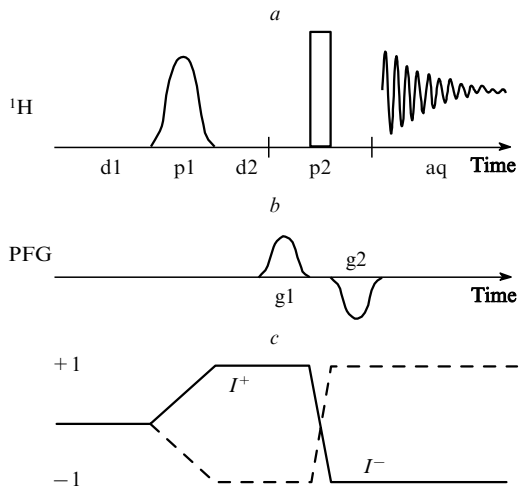


Figure 18. The RF pulse sequence (*a*), PFG sequence (*b*) and coherence pathway (*c*) in the selective gs-COSY experiment.[144]
Transition of the spin system from a lower to a higher energy level is denoted by '+1' and the reverse transition is denoted by '−1'.

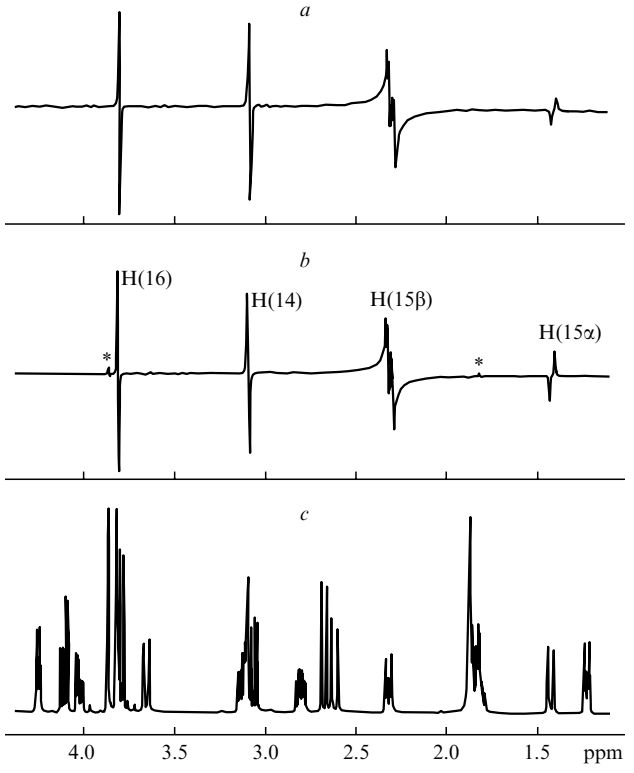


Figure 19. Brucine spectra obtained using the selective COSY sequence.[16] Selective excitation of H(14) (*a*), selective excitation of H(15β) (*b*) (residual artifacts are asterisked) and conventional selective COSY spectrum (*c*).

evolve and can be recorded. In contrast to a conventional 2D COSY experiment, selective COSY experiments allow the NMR spectrum to be recorded rather accurately, because by applying a selective pulse only one row in the COSY matrix is measured. A 'hard' 90° pulse creates a transverse magnetisation of all nuclei; therefore, their signals can be suppressed using a phase cycling scheme with a minimum number of steps (two). In particular, this concerns strong signals, *e.g.*, those of methyl or methoxyl groups, which precludes analysis of multiplet signals. The problem can be solved in the PFG experiments. Application of the gradient *g*1 causes dephasing of all coherences I^+ and I^-. A 'hard' 90° pulse acts on the I^+ and I^- coherences as follows:

$$I^+ \xrightarrow{90^\circ_x I} \frac{1}{2}(I^+ + I^-) + iI_z\,,$$

$$I^- \xrightarrow{90^\circ_x I} \frac{1}{2}(I^+ + I^-) - iI_z\,.$$

Here I^- is the observable coherence. It must be phase shifted by the negative gradient applied after the 'hard' pulse that can give rise to random artifacts in the 1D COSY spectrum. Signals created by the 'hard' pulse will be completely dephased by the second gradient.

It should be noted that gradients follow the upper trajectory (signals from the lower trajectory never reach the receiver). Therefore, gradient experiments with the same number of scans can be accompanied by a twofold decrease in signal intensity. When carrying out experiments on modern spectrometers, this is not an unsolvable problem because of rather high proton sensitivity in studies of conventional organic compounds. Another drawback of this pulse sequence is the use of a finite-duration gradient immediately before data acquisition, which leads to a large phase coefficient. The drawback can be overcome in two ways, (i) using a linear back-prediction proposed by Bernstein and Trimble [141] and (ii) by incorporating the gradient pulse into the data acquisition interval. In selective COSY experiments, an individual multiplet structure is usually of greater interest than a complete 1D NMR spectrum; therefore, it is more appropriate to adjust the phase of each multiplet individually.

2. Selective TOCSY method

Another selective excitation technique was proposed [143] for selective TOCSY experiments (Fig. 20). Initially, all protons are excited by a 'hard' 90° pulse and then dephased after the gradient pulse g1. Then, a selective RF 180° pulse changes the coherence order of the desired proton and the subsequently applied gradients g2 and g3 cause rephasing. A practical advantage of this method is that the selective 180° pulse can be calibrated much more easily than the selective 90° pulse. Moreover, it can be shown that the phase of the selective 180° pulses relative to the phase of the 'hard' pulses is of no significance. This allows the use of selective pulses

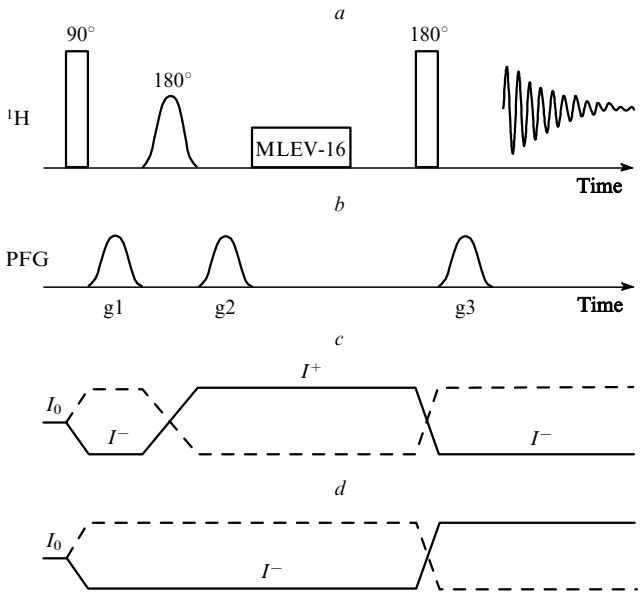


Figure 20. RF pulse sequence (*a*), PFG sequence (*b*) and the selective-pulse excited (*c*) and non-excited (*d*) coherence pathways in the gs-SELTOCSY (Selective TOCSY) experiments.

for which the carrier frequency is chosen to be slightly different from the basic frequency. Therefore, only one frequency can be used when changing the frequency range of the spectral window and all the protons under study. The second gradient is followed by the MLEV-16 spin stabilising scheme, which serves for retention of coherence order. The last gradient is rephased by applying a 'delay – 180° pulse – tailored gradient pulses' sequence. However, these methods are inappropriate for solving problems arising due to the mixing of the antiphase components within the same multiplet. As a consequence, a correct determination of the spin – spin coupling constants is complicated.

3. Double PFG echo spectroscopy

A number of methods use selective pulses and gradients for filtering unwanted magnetisations rather than excitation of particular signals. For instance, the WATERGATE technique [144] employs the pulse sequence shown in Fig. 21.

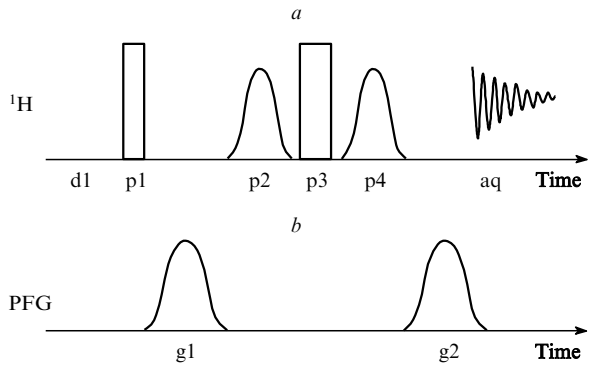


Figure 21. The RF pulse sequence (*a*) and PFG sequence (*b*) for the WATERGATE technique of water signal suppression.

To suppress an unwanted signal (often, water signal), two PFGs are applied along with a 'hard' 180° pulse (p3) and a selective 180° pulse. The last pulse is often composed of two 90° pulses, p2 and p4. Therefore the water resonance is affected by the effective 360° pulse, while all other signals are excited by the 180° pulse only, thus being influenced by two gradients of the same sign. A few versions of this method use a binomial sequence instead of selective pulses. The WATERGATE strategy was employed in some techniques known as PHOGSY (Pulse Homonuclear Gradient Spectroscopy). They permit detection of bound water molecules in proteins.[145 – 148]

Hwang and Shaka [16] showed that the use of the double pulse sequence shown in Fig. 21 improves both suppression and the phase mode; however, the 'cost' of such improvements is a decrease in the total magnetisation relaxation during the action time of two identical sets of gradient pulses.

The pulse sequence shown in Fig. 21 can be used for improving other pulsed methods. Some of them appeared to be fruitful for organic chemistry, *e.g.*, difference NOE spectroscopy. Gradient Overhauser effect spectroscopy (GOESY) [149] appeared to be a major improvement over the double pulse field gradient spin echo (DPFGSE) technique.

If the inversion rate of a molecule is such that the NOE effects become insignificant or vanish, rotating-frame experiments are usually carried out, with spins blocked by a weak RF-field. There are a number of selective methods, which also employ a spin blockade, *e.g.*, Gradient Rotation Overhauser Effect Spectroscopy (GROESY).[150] This approach is similar to the 1D TOCSY method; however, here the spin blockade is much weaker. Such sequences are included in the selective retranslated COSY scheme.[150 – 156]

4. NMR studies of C – C coupling

INADEQUATE (Incredible Natural Abundance Double Quantum Transfer Experiment) type methods are used in studies of C – C spin – spin couplings, spin system connectivities and for molecular structure analysis (in the case of long-range couplings). 2D INADEQUATE experiments are a source of valuable information in studies of organic compounds.[157] In practice, experimenters often have very small amounts of compounds under study. To obtain correct results in 2D INADEQUATE experiments, the resulting ^{13}C NMR spectrum must exhibit a signal-to-noise ratio of at least 30 : 1 after a single 90° pulse. The selective 1D INADEQUATE method is called SELINQUATE (Selective INADEQUATE);[158] it can be implemented with ease because only one row in the 2D matrix is to be measured when using a carbon-selective pulse. However, the major problem in this method is suppression of false signals from the molecules having only one ^{13}C atom. The spin – spin coupling constant ^1J(C,C) is of the order of 40 Hz and corresponding signals can be detected with ease even if the main signal is incompletely suppressed. This is insignificant if the SELINQUATE technique is used to determine the spin system connectivity, but is of crucial importance if the method is used for measuring the ^2J or ^3J constants.

The use of magnetic field gradient pulse sequences permits improvement of the INADEQUATE technique. Willker and Leibfritz [142] first demonstrated the principle used in the H,H-COSY experiments with labelled ^{13}C atoms. In this case the double-quantum filter is not employed because it nearly halves the sensitivity. The method was called GRECCO (Gradient Enhanced Measurement of Carbon Coupling);[159] the corresponding pulse sequence is shown in Fig. 22.

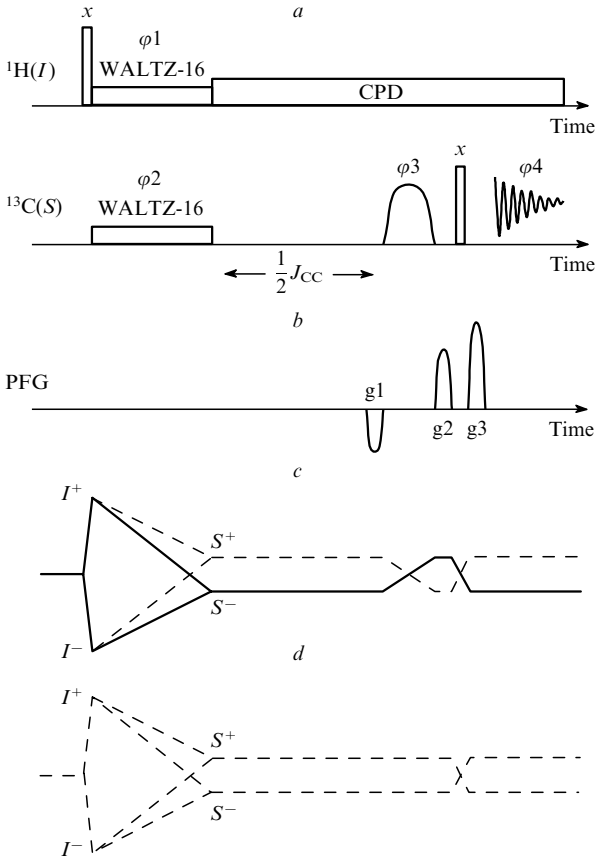


Figure 22. RF pulse sequence (*a*), PFG sequence (*b*) and the selective (*c*) and non-selective (*d*) coherence pathways in the GRECCO method. WALTZ-16 is the decoupling sequence and CPD stands for Cross Polarisation Decoupling.

The most important problem is to reduce the cross-polarisation (CP) to the desired carbon atoms. Selective inversion of coherence pathways is achieved using a Gaussian selective 180° pulse. The evolution period of duration $(1/2)J_{CC}$ (typically, 83 ms) is followed by a Gaussian 180° pulse of duration lying between 10 and 50 ms. A 'hard' 90° (^{13}C) pulse transfers the magnetisation between coupled spins. The gradient ratio $g1:g2:g3$ serves to select the magnetisations inverted by the Gaussian pulse. The corresponding coherence pathway is shown in Fig. 22*c*. The coherence pathway given in Fig. 22*d* is valid for the remaining carbon coherences; it changes under the action of three gradients. The three-gradient set provides a complete suppression. This combination of semiselective CP method and the frequency selective coherence pathway selection under the action of the 180° pulse is used to achieve selective polarisation from proton to carbon.

Weigelt and Otting [160] succeeded in suppressing all unwanted signals using PFG in proton detected INADEQUATE experiments.

An ADEQUATE (Astonishingly Sensitive Double Quantum Transfer Experiment) pulse sequence for observation of $^{13}C-^{13}C$ couplings in natural compounds has been introduced recently.[161] It permits observation of through-bond carbon–carbon couplings for up to six bonds (Fig. 23). The method provides a greater amount of information compared to, *e.g.*, the HMBC (Heteronuclear Multiple-Bond Correlation) method. Depending on the delay time, the HMBC technique allows through-bond correlations for 4–5 bonds to be observed; however, experiments with the most typical delay times of 50–80 ms make it possible to observe through-bond correlations only for 2–3 bonds. A salient feature of the ADEQUATE method is the use of adiabatic pulses with ω_1-defocussing (distribution of the components of the spin–spin coupling constants over the first dimension). This permits analysis of the spectra obtained in the same way as in the HMBC method. Some versions of this technique were successfully used for exact measurement of $^{13}C-^{13}C$ spin–spin coupling constants (see Ref. 162) and determination of ^{13}C signal multiplicities (see Ref. 163).

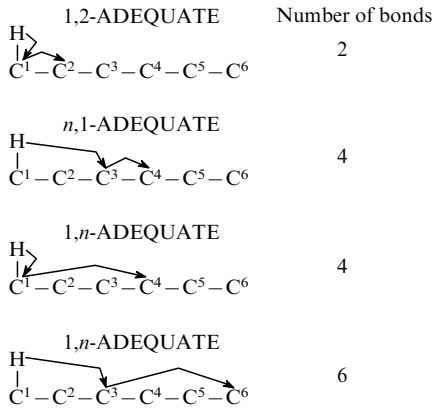


Figure 23. Scheme of correlations that can be obtained in different ADEQUATE experiments.

VIII. Heteronuclear experiments

Probing carbon nuclei allows emergence of masked proton signals. Initially, a particular carbon atom is excited and then the magnetisation is transferred to a proton, which is accompanied by significant loss of the carbon magnetisation. In this case, the main problem also consists of suppression of signals of the protons coupled to ^{13}C. Recently, numerous methods have been developed, which permit selective excitation of any proton through an appropriate coupled carbon atom and subsequent transfer of the magnetisation from the proton to the ^{13}C nucleus through scalar coupling.[161–172] The advantage of such methods is a high sensitivity.[4]

During excitation of a carbon atom under study the protons must be decoupled in order to ensure a single carbon signal and thus a high selectivity. To excite a chosen carbon atom, one must use a selective 180° pulse because it can be calibrated with ease and no phase coherence with other 'hard' carbon-selective pulses is needed.

Suppression of unwanted coherences and selective excitation of protons coupled to the chosen ^{13}C atom is more efficient in the presence of PFG. To avoid relaxation losses, the pulse sequence must be as short as possible.

An HMQC-based SELINCOR (Selective Incredible Correlation) sequence [161] (Fig. 24) is probably the first sequence including carbon-selective excitation pulses. When using the conventional inverse-INEPT sequence, the magnetisation is back-transferred to protons and the rephasing gradient 'selects' the necessary pathway.

A conventional SELINCOR module appeared to be a universal tool in the spectroscopist's hands. More recent methods (COSY,[170] TOCSY,[173] NOESY [174] and ROESY) use a selectively excited proton in order to create the 1D and 2D NMR spectra of those signals that are uncoupled from other signals. Figure 25 presents a number of spectra reported by Parella *et al.*[174]

An interesting feature is manifestation of the NOE effect between chemically equivalent protons in, *e.g.*, symmetrical

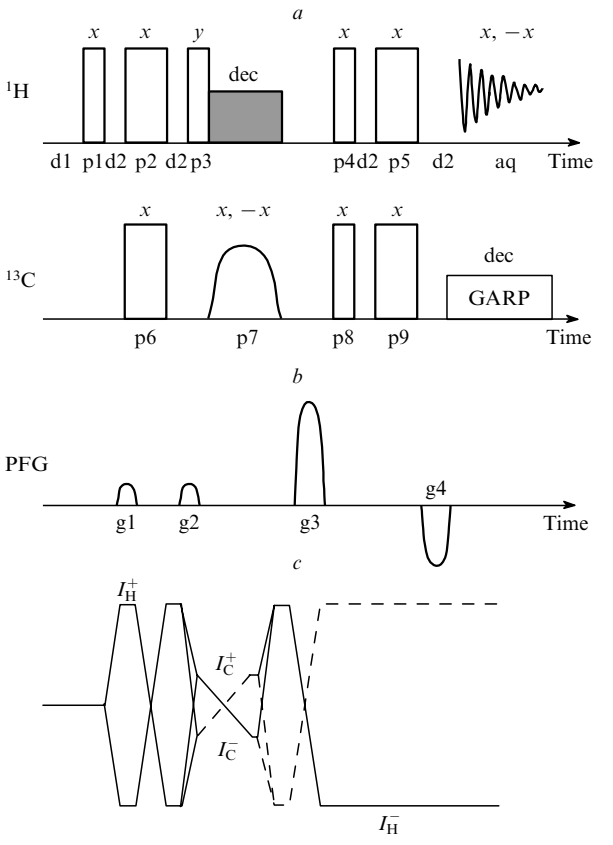


Figure 24. The RF pulse sequence (*a*), PFG sequence (*b*) and coherence pathway (*c*) in the gs-SELINCOR experiment.
The technique employs a 180° carbon selective pulse with a selected coherence pathway (solid line). d1 is the relaxation delay; p1, p3 and p4 are the 90° pulses; p2 and p5 are the 180° proton pulses; p6 and p9 are the 180° carbon pulses; p7 is the 180° carbon selective pulse; p8 is the 180° carbon pulse; g1–g4 are sinusoidal pulsed gradients; and dec is the decoupling.

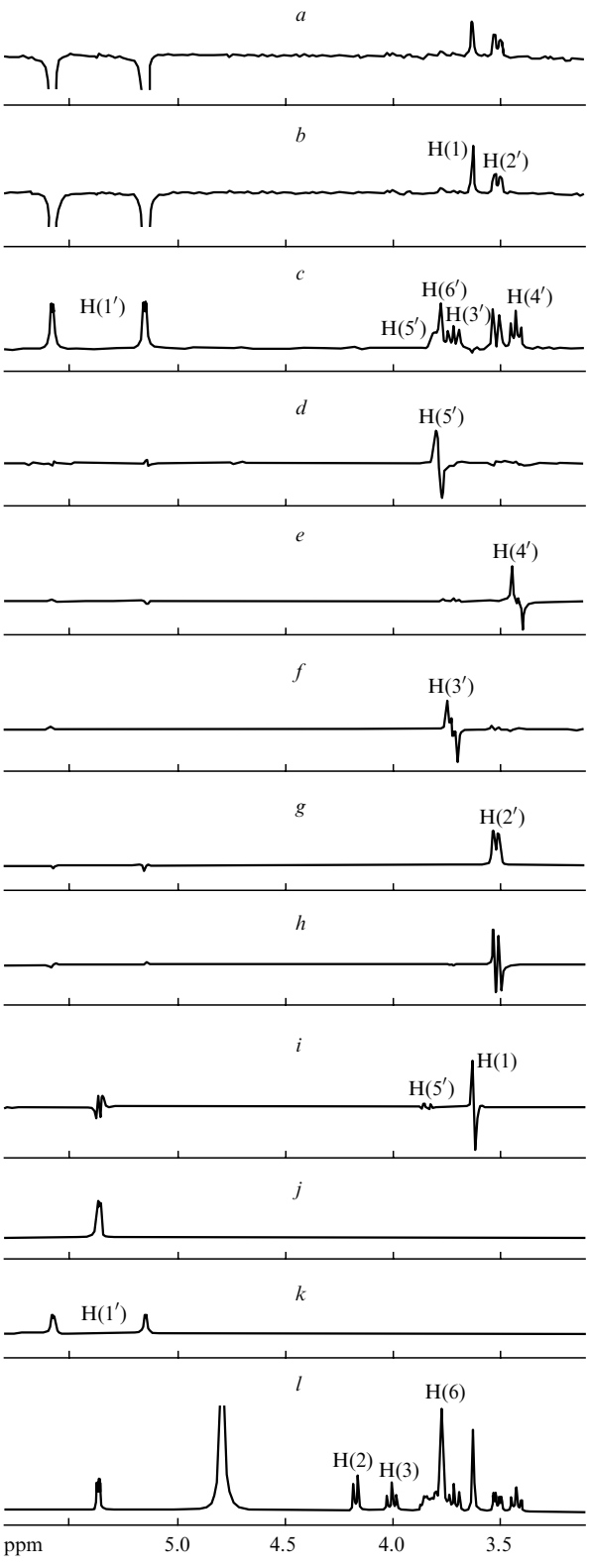


Figure 25. ^{1}H NMR spectra of saccharose obtained using different versions of the gs-HSQC pulse sequence.[174]
HSQC – ROESY (*a*), HSQC – NOESY (*b*), HSQC – TOCSY (*c*), HSQC + 2 RELAY (*d*), HSQC + 3 RELAY (*e*), HSQC + 4 RELAY (*f*), HSQC – COSY + r + z (*g*) (r is refocussing, z is filtering), HSQC – COSY (*h*), HSQC – lr (*i*) (lr is long range), HSQC/D (*j*), HSQC/C (*k*), and HSQC (*l*). The furanose and pyranose ring hydrogens are labelled by the unprimed and primed figures, respectively.

molecules. The effect can be detected using the SELINCOR technique followed by NOE transfer. Two protons can be discriminated [175] by allowing one of them to couple with ^{13}C. Pulsed field gradients can also be used provided that the spin – spin coupling constant is allowed. This permits measurement of proton – proton couplings when the proton signals are overlapped or masked by other signals.[137]

In addition to the methods shown in Fig. 25 there is yet another method of determination of the magnitude and sign of C – H coupling constants. The technique named α/β-gs-SELINCOR – TOCSY[176, 177] is a version of the approaches considered above.

The SELINCOR sequence can be modified with two 'soft' pulses. The first pulse excites a proton-decoupled carbon signal and the second one determines the spin state. The last (^{1}H) pulse in the HSQC sequence creates multiple-quantum coherences ($I^{+}S^{+}$, $I^{-}S^{+}$, $I^{+}S^{-}$ and $I^{-}S^{-}$).

The method takes into account selective creation of the coherence of the protons coupled to a particular carbon atom (in the α- or β-spin state). Then, the MLEV-16 composite pulse transfers this coherence from the protons to the carbon atom during the time interval between the second and third pulses of the TOCSY sequence. Proton coherence created using the β-gs-SELINCOR technique will be distributed over all protons belonging to the same coupled system. All proton signals are filtered and the separation between them is equal to the halved long-range H – C spin – spin coupling constant. Determination of this spin – spin coupling constant requires setting the time interval between corresponding signals.

Heteronuclear NOE effects can be useful in structural analysis of natural compounds. Traditionally, these effects are studied by either 2D HOESY spectroscopy or 1D NMR spectroscopy using selective irradiation of certain protons and measurement of the heteronuclear difference NOE spectrum. The use of magnetic field gradient pulses permits suppression of signals of the ^{12}C-coupled protons to such a degree that weak heteronuclear NOE effects will be observed in proton detection. Besides, proton detection provides a sensitivity gain. The method based on the use of both selective RF pulses and PFG was introduced by Stott and Keeler [178] and named HETGOESY (Heteronuclear Gradient Overhauser Effect Spectroscopy). The main pulse sequence employed in this technique is shown in Fig. 26. The vitality of the technique was proved in studies of gibberellic acid. The

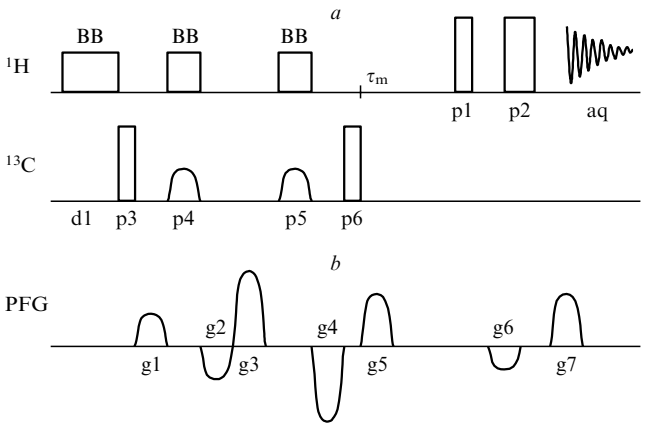


Figure 26. The RF pulse sequence (*a*) and PFG sequence (*b*) for NOE experiments with proton detection.[171]
BB is broadband decoupling; p1 and p2 are the 90° and 180° pulses, respectively; d1 is the relaxation delay; p3 and p6 are the 90° ^{13}C-pulses; p4 and p5 are the 180° ^{13}C-selective pulses; and g1 – g7 are sinusoidal pulsed gradients.

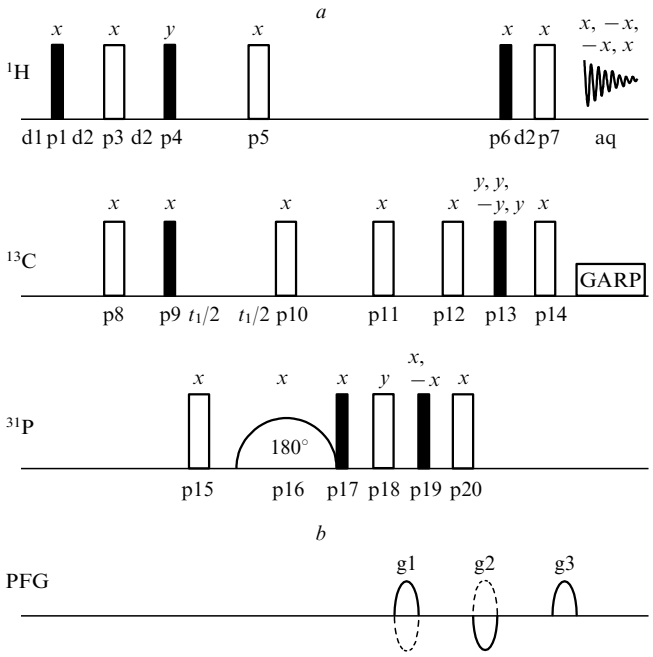


Figure 27. The RF pulse sequence (*a*) and PFG sequence (*b*) for gs-SELTRIP experiments.[182]
p16 is the 180° phosphorus selective pulse. The g1 and g2 gradients are applied in the echo – antiecho method.

approach provides a way of solving one of the most stubborn problems, namely, signal assignment of quaternary carbon atoms.

Often, the subjects of biochemical studies and investigations of organometallic compounds are molecules containing more than one atom (nucleus Y) in the heterocycle. Such molecules can be studied by 3D NMR spectroscopy using 3D ^{1}H NMR spectra and the ^{13}C and ^{31}P frequencies (see Refs 178 – 181). However, this technique is very time-consuming and offers a limited resolution. A selective triple resonance (SELTRIP) experiment [181] combines a 2D HSQC NMR technique and a selective 90° (Y) pulse in order to reduce the dimension of the problem to 2D. A modified version (gs-SELTRIP) of SELTRIP experiments is illustrated in Fig. 27.[182]

IX. Two-dimensional correlation experiments based on heteronuclear *J*-cross-polarisation

Modern versions of the HSQC method [183] can be used in multidimensional NMR experiments based on the same principles. A widely used, improved HSQC – PEP (Pulse Enhancement Polarisation) scheme [184] offers the following advantages: (i) coherence selection by PFG; (ii) a maximum sensitivity and optimisable resolution obtained by combining the echo – antiecho and PEP techniques; (iii) efficient suppression of solvent signals, achieved either using PFG (solely) or water flip-back; (iv) wide use of various pairs of NMR active nuclei; (v) applicability to both natural abundance studies of natural compounds and investigations of labelled biomolecules; and (vi) flexibility in incorporating new modules into the pulse sequence.

Design of modified HSQC techniques for selective manipulation of the spin state α and/or β has become a fruitful approach in multidimensional NMR spectroscopy. For instance, the well-known Exclusive Correlation Spectroscopy (E.COSY) [185] is widely used in the determination of homonuclear and heteronuclear spin – spin coupling constants in labelled biomolecules. To determine the sign and magnitude of very small spin – spin coupling constants, one has to measure the relative offset between cross-peaks corresponding to the spin states α and/or β in the E.COSY spectra. Recently, numerous versions of the HSQC method have been reported, which allow selection of only α or only β spin state in individual 2D NMR spectra. A simple example is provided by HSQC-α/β experiments,[186] in which the second part of the retro-INEPT pulse sequence of a conventional HSQC – PEP experiment [187] is shortened to a single 90° pulse. This shortened module selects two different coherences, one in the form of an in-phase multiplet and the second in the form of an antiphase multiplet. Simultaneous addition or subtraction of this coherence before the data acquisition stage permits selection of the α- or β-component, respectively, with retention of maximum sensitivity. This experiment allows one to obtain edited 2D correlation NMR spectra containing only one of the two multiplet signals. The spin state can be selected during the indirect evolution time; this is a coupled edited ^{1}H – X correlation NMR experiment named α/β-HSQC (or IPAP experiment).[188] The major advantage of this method is that transverse relaxation during indirect X-measurement is not as critical as in the case of ^{1}H-measurement in studies of large biomolecules. Both approaches can be combined in a single α/β-HSQC-α/β experiment, with the best example provided by the popular TROSY technique.[189] NMR experiments with editing are widely used for measuring scalar and residual dipolar coupling constants and specifying basic principles of modern NMR methods of structural and dynamics studies of large biomolecules in high-strength magnetic fields.

Correlation NMR experiments provide an attractive alternative to conventional HSQC experiments.[190] A feature of the pulse sequences proposed in that study is the use of heteronuclear cross-polarisation (HCP) for the magnetisation transfer from nucleus X to ^{1}H and/or from ^{1}H to X instead of a conventional INEPT sequence. The idea of using HCP in studies of isotropic fluids is not new. Relevant theoretical aspects have been documented (see, *e.g.*, Refs 191 and 192), including applications to protein [193] and nucleic acid studies.[194] During the last decade, analogous NMR experiments (HMQC and HSQC) have been routine tools in studies of both small molecules and large labelled and unlabelled biomolecules.

Unlike free precession ^{1}H – X-correlation experiments, HCP-experiments are based on synchronous application of two magnetic fields to both nuclei, ^{1}H (spin I) and X (spin S), and on achievement of maximum heteronuclear coherence transfer provided that the so-called Hartmann – Hahn condition is met.[195]

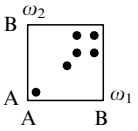
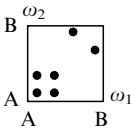
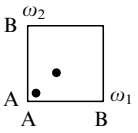
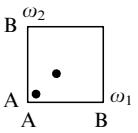
According to theoretical predictions, the HCP-based experiments [190] must exhibit a maximum sensitivity due to selection and combination of two different magnetisations. The anisotropy of heteronuclear coherence transfer involving HCP mixing processes is demonstrated by strong dependence of the transfer mechanism on the relative phase between the input magnetisation and the HCP mixing sequence. A number of similar pulse schemes have been designed for simple and selective manipulation of various coherences available before and after the HCP mixing. Such schemes are characterised by high sensitivity, good stability to RF field inhomogeneities, better (compared to HSQC experiments) behaviour of the spin system in the relaxation and chemical exchange processes, versatility and possibility of being slightly modified.

The use of novel, optimised, ultrabroadband heteronuclear cross-polarisation sequences including improved multiple-pulse sequences or adiabatic pulses and HCP-based strategies presents an alternative to the most popular HSQC pulse schemes. In addition, various HCP modules can be incorporated into multidimensional NMR experiments as efficient preparation and mixing modules.

X. Combined use of selective and non-selective excitation in NMR experiments

A method of studying molecular dynamics processes was proposed.[196] The technique involves excitation of a single nucleus in a coupled spin system using the Multiplet-Selective Excitation (MUSEX) pulse sequence.[197] The usefulness of the method

Table 5. Versions of the MUSEX COSY technique.[196]

Version	Pulse sequence	2D spectral pattern
NSP – SP(A) MUSEX COSY	$90^\circ_x - t_1 - 90^\circ_x(\mathrm{A}) - t_2$	
SP(A) – NSP MUSEX COSY	$90^\circ_x(\mathrm{A}) - t_1 - 90^\circ_x - t_2$ $\sigma_4^{\mathrm{expl}} = I_{\mathrm{A}y} S^1_{\mathrm{A}} C^1_J S^2_{\mathrm{A}} C^2_J +$ $+ I_{\mathrm{B}y} S^1_{\mathrm{A}} S^1_J S^2_{\mathrm{B}} S^2_J - I_{\mathrm{B}y} C^2_{\mathrm{B}} C^2_J$	
SP(A) – SP(A) MUSEX COSY	$90^\circ_x(\mathrm{A}) - t_1 - 90^\circ_x(\mathrm{A}) - t_2$ $\sigma_4^{\mathrm{expl}} = I_{\mathrm{A}y} C^1_{\mathrm{A}} S^1_{\mathrm{A}} C^2_{\mathrm{A}} S^2_J +$ $+ I_{\mathrm{A}y} S^1_{\mathrm{A}} C^1_J S^2_{\mathrm{B}} C^2_J$	
SP(A) – SP(B) MUSEX COSY	$90^\circ_x(\mathrm{A}) - t_1 - 90^\circ_x(\mathrm{B}) - t_2$ $\sigma_4^{\mathrm{expl}} = -I_{\mathrm{A}y} C^1_{\mathrm{A}} C^1_J C^2_{\mathrm{A}} C^2_J +$ $+ I_{\mathrm{A}y} S^1_{\mathrm{A}} C^1_J S^2_{\mathrm{B}} C^2_J - I_{\mathrm{B}y} C^2_{\mathrm{B}} C^2_J$	

Note. Here and in Table 6 we use the following notations: NSP is the non-selective pulse; SP(A(B)) is the selective pulse exciting the A or B nuclei, respectively; $C^{1(2),\tau}_{\mathrm{A(B)}} = \cos \Omega_{\mathrm{A(B)}} t_{1(2)}$; $C^{1(2),\tau}_J = \cos \pi J_{\mathrm{AB}} t_{1(2)}$; $S^{1(2),\tau}_{\mathrm{A(B)}} = \sin \Omega_{\mathrm{A(B)}} t_{1(2)}$; $S^{1(2),\tau}_J = \sin \pi J_{\mathrm{AB}} t_{1(2)}$; filled circles in the 2D spectral patterns denote positive intensity; t_1 and t_2 are variable time intervals, and τ is a constant time interval.

consists of minimisation of information loss on the spin – spin coupling, which favours simplification of detection technique and signal assignment in spin systems. This requires experiments with combined selective and non-selective excitation.

Consider the behaviour of a weakly coupled AB spin system under the action of a two-pulse MUSEX COSY sequence.[196] The case of two non-selective pulses presents a well-known conventional COSY experiment.[4, 197] It is of interest to consider all possible combinations of selective and non-selective pulses. Table 5 schematically depicts 2D NMR spectra with explicitly observable components.

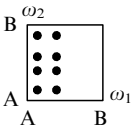
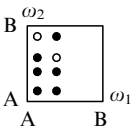
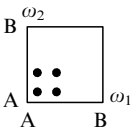
NSP – SP(A) MUSEX COSY experiments allow the NMR spectral pattern to be simplified without loss of information on the spin – spin coupling (here, *J*-cross-peaks are absent because of selective excitation).

The SP(A) – SP(A) MUSEX COSY technique can be implemented in EXSY experiments used in chemical exchange studies.

The SP(A) – SP(B) MUSEX COSY method can be useful for obtaining information on the spin – spin coupling between any two spins in a multiple-spin system.

Non-selective NMR spectra often include a number of regions with overlapped multiplet signals, which leads to ambiguity in the interpretation of such spectra. A particular value of the approach [196] is the possibility of avoiding this ambiguity. MUSEX experiments allow the size of the data array to be reduced and the duration of experiments to be shortened. The techniques mentioned above are applicable to all types of 2D experiments. Table 6 lists all observable components for spin A and provides their schematic representation in the form of a 2D NMR spectrum for the three-pulse sequences containing a complete set of possible combinations of non-selective and multiplet-selective pulses. Excitation of spin B gives rise to an axial doublet in the NMR spectrum. A distinctive feature of the experiments consists of the use of alternating spin excitation (ALEX) using the MUSEX

Table 6. 2D subspectral patterns.[196, 198]

Number	Pulse sequence	2D spectral pattern
1	$90^\circ_x(\mathrm{B}) - t_1 - 90^\circ_x(\mathrm{A}) - \tau - 90^\circ_x(\mathrm{A}) - t_2$	
2	$90^\circ_x(\mathrm{A}) - t_1 - 90^\circ_x(\mathrm{A}) - \tau - 90^\circ_x(\mathrm{B}) - t_2$	
3	$90^\circ_x(\mathrm{B}) - t_1 - 90^\circ_x(\mathrm{B}) - \tau - 90^\circ_x(\mathrm{A}) - t_2$	

Note. Open circles in the 2D spectral patterns denote negative intensity.

sequence. All calculations were carried out using the operator product formalism, as in the MUSEX COSY method.

The pulse sequences *1* and *2* allow visualisation of each coupling in a multiplet system. The pulse sequence *1* can be used in a stepwise manner for identification of all coupled partners in a complex spin system, because the MUSEX COSY experiments allow all couplings to be followed simultaneously. The pulse sequence *2* is convenient for studying relaxation mechanisms. The resulting NMR spectrum (pulse sequence *3*) exhibits a spin-A diagonal peak appearing as a result of interference of eight components, of which four components are single-quantum coherences and the remaining components were transferred from double-quantum and zero-quantum coherences. In this case the first two pulses represent the ALEX COSY technique and the last B-nucleus pulse is used as the detection pulse. With an appropriately adjusted phase, two resonance lines for the diagonal peaks can disappear, thus leaving only diagonal lines.

* * *

At present, NMR spectroscopy offers a variety of methods which permit identification and investigation of the structure and dynamics of complex biomolecules and biosystems. Advantages in these studies are to a great extent due to both design of new hardware and the use of various selective methods. Combining radiofrequency pulses and magnetic field gradient pulses allowed a number of problems arising in the experiments with selective pulses (in particular, the problem of selection of desired coherences) to be solved. One can expect that some of these methods will become routine techniques in NMR spectroscopy of organic compounds, because often they give a fast and detailed answer to those questions that were unanswerable a few years ago.

The review has been written with the financial support of the Russian Foundation for Basic Research (Project Nos 03-03-32296, 04-03-96807 and 04-03-81028).

References

1. R R Ernst, in *Nuclear Magnetic Resonance Fourier Transform Spectroscopy. Nobel Lecture. The 9th December, 1991* Prix Nobel, 1992, p. 70
2. J W Emsley, J Feeney, L H Sutcliffe *High Resolution Nuclear Magnetic Resonance Spectroscopy* (Oxford: Pergamon Press, 1965)
3. J H Noggle, R E Schirmer *The Nuclear Overhauser Effect, Chemical Application* (Oxford: Academic Press, 1971)

4. R R Ernst, G Bodenhausen, A Wokaun *Principles of Nuclear Magnetic Resonance in One and Two Dimensions* (Oxford: Clarendon Press, 1987)
5. D Neuhaus, M P Williamson *The Nuclear Overhauser Effect in Structural and Conformational Analysis* (New York: VCH, 1989)
6. W R Croasmun, R M K Charlson *Two-Dimensional NMR Spectroscopy. Application for Chemists and Biochemists* (Second Ed.) (New York: VCH, 1994)
7. M Spraul, J K Nicholson, M J Lynch, J C Lindon *J. Pharm. Biomed. Anal.* **12** 5 613 (1994)
8. S Warren, S M Silver *Adv. Magn. Reson.* **12** 247 (1988)
9. H Kessler, S Mronga, G Gemmecker *Magn. Reson. Chem.* **29** 527 (1991)
10. L Emsley *Methods Enzymol.* **239** 207 (1994)
11. T J Norwood *Chem. Soc. Rev.* **23** 59 (1994)
12. J Keeler, R T Clowes, A L Davis, E D Laue *Methods Enzymol.* **239** 145 (1994)
13. W I Price *Ann. Rep. NMR* **32** 51 (1996)
14. T Parella *Magn. Reson. Chem.* **34** 329 (1996)
15. V Blechta, R Freeman *J. Magn. Reson., Ser. A* **102** 253 (1993)
16. T-L Hwang, A J Shaka *J. Magn. Reson., Ser. A* **112** 275 (1995)
17. J Friedrich, S Davies, R Freeman *J. Magn. Reson.* **75** 390 (1987)
18. Yu E Chernysh, G S Borodkin, B S Luk'yanov, M S Korobov, Yu M Korobov, V Yu Vdovichenko, N V Stankevich *Selektivnaya Fur'e-spektroskopiya YaMR i ee Prilozhenie k Issledovaniyu Protsessov Molekulyarnoi Dinamiki* (Selective Fourier Transform Nuclear Magnetic Resonance Spectroscopy and Its Application to Investigation of the Processes of Molecular Dynamics) (Rostov-on-Don: Izd. SKNTs Vyssh. Shk., 2002)
19. S Braun, H O Kalinowski, S Berger *100 and More Basic NMR Experiments* (Weinheim: VCH, 1996)
20. S L Patt, J N Shoolery *J. Magn. Reson.* **46** 535 (1982)
21. H Bildsoe, S Donstrup, H J Jakobsen, O W Sorensen *J. Magn. Reson.* **53** 154 (1983)
22. O W Sorensen, S Donstrup, H Bildsoe, H J Jakobsen *J. Magn. Reson.* **55** 347 (1983)
23. J M Bulsing, W M Brooks, J Field, D M Doddrell *J. Magn. Reson.* **56** 167 (1984)
24. J M Bulsing, D M Doddrell *J. Magn. Reson.* **61** 197 (1985)
25. G A Morris, R Freeman *J. Am. Chem. Soc.* **101** 760 (1979)
26. D P Burum, R R Ernst *J. Magn. Reson.* **39** 163 (1980)
27. D T Pegg, D M Doddrell, M R Bendall *J. Chem. Phys.* **77** 2745 (1982)
28. D M Doddrell, D T Pegg, M R Bendall *J. Magn. Reson.* **48** 323 (1982)
29. O W Sorensen, R R Ernst *J. Magn. Reson.* **51** 477 (1983)
30. J Homer, M C Perry *J. Chem. Soc., Chem. Commun.* 373 (1994)
31. M H Levitt, O W Surensen, R R Ernst *Chem. Phys. Lett.* **94** 540 (1983)
32. L Muller *J. Am. Chem. Soc.* **101** 4481 (1979)
33. H Kessler, P Schmieder, M Kurz *J. Magn. Reson.* **85** 400 (1989)
34. U Wolborn, T Domke, D Leibfritz *J. Magn. Reson.* **90** 575 (1990)
35. T Domke, D Leibfritz *J. Magn. Reson.* **88** 401 (1990)
36. H Kessler, P Schmieder, M Kuck, M Reggelin *J. Magn. Reson.* **91** 375 (1991)
37. T Domke, P Xu, R Freeman *J. Magn. Reson.* **92** 218 (1991)
38. U Wolborn, D Leibfritz, T Domke *J. Magn. Reson.* **94** 653 (1991)
39. D Davis *J. Magn. Reson.* **90** 589 (1990)
40. W Willker, J Stelten, D Leibfritz *J. Magn. Reson., Ser. A* **107** 94 (1994)
41. J M Schmidt, H Rueterjans *J. Am. Chem. Soc.* **112** 1279 (1990)
42. A Steck, P Bigler *J. Magn. Reson., Ser. A* **110** 90 (1994)
43. M L Liu, R D Farrant, J K Nicholson, J C Lindon *J. Magn. Reson., Ser. B* **106** 270 (1995)
44. M L Liu, R D Farrant, J K Nicholson, J C Lindon *J. Magn. Reson., Ser. A* **112** 208 (1995)
45. M L Liu, R D Farrant, B C Sweatman, J K Nicholson, J C Lindon *J. Magn. Reson., Ser. A* **113** 251 (1995)
46. M L Liu, R D Farrant, J K Nicholson, J C Lindon *Magn. Reson Chem.* **33** 212 (1995)
47. M L Liu, J K Nicholson, J C Lindon, P N Sanderson, G E Tranter *Magn. Reson. Chem.* **34** 865 (1996)
48. H Kessler, P Schmieder *Biopolymers* **31** 621 (1991)
49. G E Martin, R C Crouch *J. Nat. Prod.* **54** 1 (1991)
50. T Parella *Magn. Reson. Chem.* **36** 467 (1998)
51. G Bodenhausen, R L Vold, R R Vold *J. Magn. Reson.* **37** 93 (1980)
52. J Stelten, D Leibfritz *J. Magn. Reson.* **99** 170 (1992)
53. M L Liu, H R Tang, J K Nicholson, J C Lindon *Magn. Reson. Chem.* **40** 83 (2002)
54. M H Levitt, R Freeman *J. Magn. Reson.* **39** 533 (1980)
55. L Braunschweiler, R R Ernst *J. Magn. Reson.* **53** 521 (1983)
56. D J Cookson, B E Smith *Org. Magn. Reson.* **16** 111 (1981)
57. M R Bendall, D M Doddrell, D T Pegg *J. Am. Chem. Soc.* **103** 4603 (1981)
58. W S Price *Ann. Rep. NMR* **38** 289 (1999)
59. A Bax, D G Davis, *J. Magn. Reson.* **65** 355 (1985)
60. W P Aue, J Karhan, R R Ernst *J. Chem. Phys.* **64** 4226 (1976)
61. J K Nicholson, I D Wilson *Prog. Nucl. Magn. Reson. Spectrosc.* **21** 449 (1989)
62. A Bax, R Freeman, G A Morris *J. Magn. Reson.* **43** 333 (1981)
63. A Bax, A F Mehlkopf, J Smidt *J. Magn. Reson.* **35** 167 (1979)
64. M P Williamson *J. Magn. Reson.* **55** 471 (1983)
65. P Xu, X Wu, R Freeman *J. Magn. Reson.* **95** 132 (1991)
66. A J Shaka, J Keeler, R Freeman *J. Magn. Reson.* **56** 294 (1984)
67. M Woodley, R Freeman *J. Magn. Reson., Ser. A* **109** 103 (1994)
68. G W Vuiste, R Boelens *J. Magn. Reson.* **73** 328 (1987)
69. M L Woodley, T A Carpenter, L D Hall *J. Magn. Reson., Ser. A* **106** 147 (1994)
70. M Karplus *J. Chem. Phys.* **30** 11 (1959)
71. V F Bystrov *Prog. Nucl. Magn. Reson. Spectrosc.* **10** 41 (1976)
72. G Xu, C M Deber *Int. J. Peptide Protein Res.* **37** 528 (1991)
73. J L Nietro, M Rico, J Santoro, J Herranz, F J Bermejo *Int. J. Pep. Protein Res.* **28** 315 (1986)
74. M L Liu, X A Mao, in *Encyclopedia of Spectroscopy and Spectrometry* (Eds J C Lindon, J M Holmes, G E Tranter) (San Diego, CA: Academic Press, 1999) p. 2145
75. M Liu, J C Lindon *Curr. Org. Chem.* **5** 351 (2001)
76. E O Stejskal, J E Tanner *J. Chem. Phys.* **42** 288 (1965)
77. J E Tanner *J. Phys. Chem.* **52** 2523 (1970)
78. C S Johnson Jr *Prog. Nucl. Magn. Reson. Spectrosc.* **34** 203 (1999)
79. J S Gounarides, A D Chen, M J Shapiro *J. Chromatogr. B* **725** 79 (1999)
80. A D Chen, M J Shapiro *Anal. Chem.* **71** 669A (1999)
81. M Liu, J K Nicholson, J A Parkinson, J C Lindon *Anal. Chem.* **69** 1504 (1997)
82. D P Hinton, C S Johnson Jr *J. Phys. Chem.* **97** 9064 (1993)
83. A Chen, D Wu, C S Johnson Jr *J. Am. Chem. Soc.* **117** 7965 (1995)
84. D P Hinton, C S Johnson Jr *Chem. Phys. Lipids* **69** 175 (1994)
85. H Barjat, G A Morris, S Smart, A G Swanson, S C R Williams *J. Magn. Reson., Ser. B* **108** 170 (1995)
86. A S Altieri, D P Hinton, R A Byrd *J. Am. Chem. Soc.* **117** 7566 (1995)
87. M F Lin, C K Larive *Anal. Biochem.* **229** 214 (1995)
88. R F Karlicek Jr , I J Lowe *J. Magn. Reson.* **37** 75 (1980)
89. R M Cotts, M J R Hoch, T Sun, J T Markert *J. Magn. Reson.* **83** 252 (1989)
90. G H Sørland, D Aksnes, L Gjerdaker *J. Magn. Reson.* **137** 397 (1999)
91. H Y Carr, E M Purcell *Phys. Rev.* **94** 630 (1954)
92. N M Loening, J Keeler *J. Magn. Reson.* **139** 334 (1999)
93. A Jerschow, N Müller *J. Magn. Reson.* **125** 372 (1997)
94. A Jerschow, N Müller *J. Magn. Reson.* **132** 13 (1998)
95. S J Gibbs, C S Johnson Jr *J. Magn. Reson.* **93** 395 (1991)
96. J Ruiz-Cabello, G W Vuister, C T W Moonen, P Van Gelderen, J S Cohn, P C M Van Zijl *J. Magn. Reson.* **100** 282 (1992)
97. E Kupce, R Freeman *J. Biomol. NMR* **25** 349 (2003)
98. S Meiboom, D Gill *Rev. Sci. Instrum.* **29** 688 (1958)
99. T Gullion, D B Baker, M S Corradi *J. Magn. Reson.* **89** 479 (1990)
100. D H Wu, A D Chen, C S Johnson Jr *J. Magn. Reson., Ser. A* **115** 260 (1995)
101. In *Bruker Almanac. NMR Tables, 1998* p. 69
102. J K Nicholson, P D Foxall, M Spraul, R D Farrant, J C Lindon *Anal. Chem.* **67** 793 (1995)
103. M Liu, J K Nicholson, J C Lindon *Anal. Chem.* **68** 3370 (1996)

104. A Chen, D Wu, C S Johnson Jr *J. Phys. Chem.* **99** 828 (1995)
105. A K Gaigalas, J B Hubbard, M McCurley, S Woo *J. Phys. Chem.* **96** 2355 (1992)
106. M Liu, H C Toms, G E Hawkes, J K Nicholson, J C Lindon *J. Biomol. NMR* **13** 25 (1999)
107. M Liu, J K Nicholson, J C Lindon *Anal. Commun.* **34** 225 (1997)
108. M Liu, J K Nicholson, J A Parkinson, J C Lindon *Anal. Chem.* **69** 1504 (1996)
109. D Wu, A Chen, C S Johnson Jr *J. Magn. Reson. A* **121** 88 (1996)
110. E K Gosansky, D G Gorenstein *J. Magn. Reson. B* **111** 94 (1996)
111. D Wu, A Chen, C S Johnson Jr, in *Abstracts of the 37th ENC, Asilomar, CA, 1996* p. 74
112. B E Chapman, P W Kuchel *J. Magn. Reson., Ser. A* **102** 105 (1993)
113. S J Gibbs, C S Johnson Jr *J. Magn. Reson.* **93** 395 (1991)
114. J Chen, A A De Angelis, V A Mandelshtam, A J Shaka *J. Magn. Reson.* **162** 74 (2003)
115. D Zax, A Pines *J. Chem. Phys.* **78** 6333 (1983)
116. C H Sotak *NMR Biomed.* **4** 70 (1991)
117. C H Sotak *J. Magn. Reson.* **90** 198 (1990)
118. E Mischler, F Humber, B Diter, D Canet *J. Magn. Reson., Ser. B* **106** 32 (1995)
119. P Mutzenhardt, D Canet *J. Chem. Phys.* **105** 4405 (1996)
120. P W Kuchel, B E Chapman *J. Magn. Reson., Ser. A* **101** 53 (1993)
121. M Liu, X-A Mao, C Ye, J K Nicholson, J C Lindon *J. Magn. Reson.* **129** 67 (1997)
122. S Kim, T Szyperski *J. Am. Chem. Soc.* **125** 1385 (2003)
123. X Zhang, C-G Li, C-H Ye, M-L Liu *Anal. Chem.* **73** 3528 (2001)
124. E Kupce, R Freeman *J. Magn. Reson.* **163** 56 (2003)
125. M Liu, X-A Mao, C Ye, J K Nicholson, J C Lindon *Mol. Phys.* **93** 913 (1998)
126. S Altieri, K E Miller, R A Byrd *Magn. Reson. Rev.* **17** 27 (1996)
127. H Weingartner, M Holz *Annu. Rep. Prog. Chem., Sect. C* **98** 121 (2002)
128. M J Thrippleton, N M Loening, J Keeler *Magn. Reson. Chem.* **41** 441 (2003)
129. R J Ogg, R B Kingsley, J S Taylor *J. Magn. Reson., Ser. B* **104** 1 (1994)
130. V Sklenar, M Piotto, R Leppik, V Saudek *J. Magn. Reson., Ser. A* **102** 241 (1993)
131. M Liu, X A Mao, C H Ye, H Huang, J K Nicholson, J C Lindon *J. Magn. Reson.* **132** 125 (1998)
132. W S Price, K Hayamizu, Y Arata *J. Magn. Reson.* **126** 256 (1997)
133. W Kozminski, I Zhukov *J. Biomol. NMR* **26** 157 (2003)
134. P C M Van Zijl, C T W Moonen *J. Magn. Reson.* **87** 18 (1990)
135. S Connor, J K Nicholson, J R Everett *Anal. Chem.* **59** 2885 (1987)
136. D B Fulton, R Hrabal, F Ni *J. Biomol. NMR* **8** 213 (1996)
137. S Berger *Prog. Nucl. Magn. Reson. Spectrosc.* **30** 137 (1997)
138. M Liu, H Tang, J K Nicholson, J C Lindon *J. Magn. Reson.* **153** 133 (2001)
139. C Dhalluin, J-M Wieruszeski, G Lippens *J. Magn. Reson., Ser. B* **111** 168 (1996)
140. P Adell, T Parella, F Sanchez-Ferrando, A Virgili *J. Magn. Reson., Ser. B* **108** 77 (1995)
141. M A Bernstein, L A Trimble *Magn. Reson. Chem.* **32** 107 (1994)
142. W Willker, D Leibfritz *Magn. Reson. Chem.* **32** 665 (1994)
143. T Facke, S Berger *J. Magn. Reson., Ser. A* **113** 257 (1995)
144. M Piotto, V Saudek, V Sklenar *J. Biomol. NMR* **2** 661 (1992)
145. E Kupce, R Freeman *J. Biomol. NMR* **28** 391 (2004)
146. L A Trimble, M A Bernstein *J. Magn. Reson., Ser. B* **105** 67 (1994)
147. C Dalvit, U Hommel *J. Magn. Reson., Ser. B* **109** 334 (1995)
148. K Stott, J Stonehouse, J Keeler, T-L Hwang, A J Shaka *J. Am. Chem. Soc.* **117** 4199 (1994)
149. J Stonehouse, P Adell, J Keeler, A J Shaka *J. Am. Chem. Soc.* **116** 6037 (1994)
150. P Adell, T Parella, F Sanchez-Ferrando, A Virgili *J. Magn. Reson., Ser. A* **113** 124 (1995)
151. O W Sørensen, G H Eich, M H Levitt, G Bodenhausen, R R Ernst *Prog. Nucl. Magn. Reson. Spectrosc.* **16** 163 (1984)
152. J R Garbow, D P Weitekamp, A Pines *Chem. Phys. Lett.* **93** 504 (1982)
153. D G Davis *J. Magn. Reson., Ser. B* **101** 229 (1993)
154. M Gueron, P Plateau, in *Encyclopedia of Nuclear Magnetic Resonance* (Eds D M Grant, R K Harris) (New York: Wiley, 1996) p. 4931
155. C Dalvit *J. Magn. Reson., Ser. A* **113** 120 (1995)
156. C Dalvit, S Y Ko, J M Bohlen *J. Magn. Reson., Ser. B* **110** 124 (1996)
157. J Buddrus, H Bauer *Angew. Chem. Int. Ed. Engl.* **26** 625 (1987)
158. S Berger *Angew. Chem. Int. Ed. Engl.* **27** 1196 (1988)
159. T Fäcke, S Berger *J. Am. Chem. Soc.* **117** 9547 (1994)
160. J Weigelt, G Otting *J. Magn. Reson., Ser. A* **113** 128 (1995)
161. M Köck, R Kerssebaum, W Bermel *Magn. Reson. Chem.* **41** 65 (2003)
162. K Kövér, P Forgd *J. Magn. Reson.* **166** 47 (2004)
163. T Parella, F Sanchez-Ferrando *J. Magn. Reson.* **166** 123 (2004)
164. S Berger *J. Magn. Reson.* **81** 561 (1989)
165. M Ochs, S Berger *Magn. Reson. Chem.* **28** 994 (1990)
166. R C Crouch, J P Shockor, G E Martin *Tetrahedron Lett.* **31** 5273 (1990)
167. P Berthault, B Perly, M Petitou *Magn. Reson. Chem.* **28** 696 (1990)
168. M J Crossley, L D Field, J J Gosper, B A Messerle *Magn. Reson. Chem.* **25** 297 (1987)
169. K Ding, A Gronenborn *J. Magn. Reson.* **156** 262 (2002)
170. T Facke, S Berger *Magn. Reson. Chem.* **33** 144 (1995)
171. K Zangger, H Sterk *Magn. Reson. Chem.* **33** 577 (1995)
172. R Wagner, S Berger *Fresenius' J. Anal. Chem.* **357** 470 (1997)
173. T Facke, S Berger *Tetrahedron* **51** 3521 (1995)
174. T Parella, F Sanchez-Ferrando, A Virgili *J. Magn. Reson., Ser. A* **114** 32 (1995)
175. R Wagner, S Berger *Magn. Reson. Chem.* **35** 199 (1997)
176. T Facke, S Berger *J. Magn. Reson., Ser. A* **119** 260 (1996)
177. M Eberstadt, G Gemmecker, D F Mierke, H Kessler *Angew. Chem., Int. Ed. Engl.* **34** 1671 (1995)
178. K Stott, J Keeler *Magn. Reson. Chem.* **34** 554 (1996)
179. S Berger, P Bast *Magn. Reson. Chem.* **31** 1021 (1993)
180. H A Heus, S S Wijmenga, F J M van de Ven, C W Hilbers *J. Am. Chem. Soc.* **116** 4983 (1994)
181. J P Marino, H Schwalbe, C Anklin, W Bermel, D M Crothners, C Griesinger *J. Am. Chem. Soc.* **116** 6472 (1994)
182. R Wagner, S Berger *J. Magn. Reson., Ser. A* **120** 258 (1996)
183. G Bodenhausen, D J Ruben *Chem. Phys. Lett.* **69** 185 (1980)
184. L E Kay, P Keifer, T J Saarinen *J. Am. Chem. Soc.* **114** 10663 (1992)
185. C Griesinger, O W Sorensen, R R Ernst *J. Am. Chem. Soc.* **107** 6394 (1985)
186. M D Sorensen, A Meissner, O W Sorensen *J. Magn. Reson.* **137** 237 (1999)
187. A G Palmer III, J Cavanagh, P E Wright, M Rance *J. Magn. Reson.* **93** 151 (1991)
188. M Ottiger, F Delaglio, A Bax *J. Magn. Reson.* **131** 373 (1998)
189. T Schulte-Herbrüggen, T S Untidt, N C Nielsen, O W Sorensen *J. Chem. Phys.* **115** 8506 (2001)
190. T Parella *J. Biomol. NMR* **29** 37 (2004)
191. S Glaser, J J Quant, in *Advances in Magnetic and Optical Resonance* Vol. 19 (Ed. W S Warren) (New York: Academic Press, 1996) p. 59
192. M Ernst, C Griesinger, R R Ernst, W Bermel *Mol. Phys.* **74** 219 (1991)
193. E R P Zuiderweg, L Zeng, B Brutscher, R C Morshauser *J. Biomol. NMR* **8** 147 (1996)
194. V Sklenar, T Dieckmann, S E Butcher, J Feigon *J. Biomol. NMR* **7** 83 (1996)
195. S R Hartmann, E L Hahn *Phys. Rev.* **128** 2042 (1962)
196. Yu E Chernysh, G S Borodkin, E V Sukholenko, L E Nivorozhkin *J. Magn. Reson.* **96** 131 (1992)
197. Ch J Turner *Prog. NMR Spectrosc.* **16** 311 (1984)
198. Yu E Chernysh, G S Borodkin, L E Nivorozkin *Appl. Magn. Reson.* **5** 69 (1993)